https://rbgeomorfologia.org.br/
ISSN 2236-5664

Revista Brasileira de Geomorfologia

v. 26, nº 4 (2025)

https://dx.doi.org/10.20502/rbg.v26i4.2716

Research Article

The Protective Function of Coastal Habitats in Mitigating Erosive Vulnerability: A Case Study on Sandy Beaches of the Equatorial Atlantic, Northeastern Brazil

Função Protetiva de Habitats Costeiros na Mitigação da Vulnerabilidade Erosiva: Estudo de Caso em Praias Arenosas do Atlântico Equatorial, Nordeste do Brasil

Gabriel Dalla Rosa Carvalho[1], Venerando Eustáquio Amaro[2], Lívian Rafaely de Santana Gomes Pinheiro[3], Nadia Selene Zamboni[4]

[1] Federal University of Rio Grande do Norte, Postgraduate Program in Civil and Environmental Engineering, Natal, Brazil. gabrieldrcarvalho@gmail.com
ORCID: https://orcid.org/0009-0005-2026-5211

[2] Federal University of Rio Grande do Norte, Department of Civil and Environmental Engineering, Natal, Brazil. venerando.amaro@gmail.com
ORCID: https://orcid.org/0000-0001-7357-2200

[3] Federal Unifersity of Ceará, Department of Geology, Fortaleza, Brazil. livianrafaely@gmail.com
ORCID: https://orcid.org/0000-0001-6606-8807

[4] Federal University of Rio Grande do Norte, Laboratory of Applied Geotechnologies, Coastal and Oceanic Modeling, Natal, Brazil. nselenezamboni@gmail.com
ORCID: https://orcid.org/0000-0002-7828-5910

Received: 22/06/2025; Accepted: 10/11/2025; Published: 09/12/2025

Abstract: Coastal environments are subject to intense pressure from both natural and anthropogenic factors, often culminating in landscape alterations such as sandy beach erosion. On the northern coast of Rio Grande do Norte (RN), rapid urban and tourist expansion has intensified these processes. This study assesses coastal vulnerability to erosion along sandy beaches segments in the municipality of São Miguel do Gostoso (RN), considering the protective function of natural habitats, specifically dunes, vegetation, and beach stretches. The methodology is based on remote sensing and geoprocessing data, involving the examination of historical shoreline variation from 1986 to 2023, as the application of the Coastal Vulnerability Index via the Integrated Valuation of Environmental Services and Tradeoffs (InVEST) model. The results indicate an increase in mean shoreline mobility during the more recent period (2014–2023), with intensified minimum and maximum rates of variation, particularly in areas subjected to greater anthropogenic influence, where the average erosion rate reaches -14.55 m/year. It was further found that dunes and sandy beaches function as effective natural barriers, thereby reducing erosion. The conservation of these habitats is essential for the environmental balance of the coastal zone, especially in the face of increasing urban expansion in the municipality.

Keywords: Coastal infrastructures; InVEST; Hydro-sedimentary modeling; Coastal land use and cover.

Resumo: Os ambientes costeiros estão sujeitos à intensa pressão de fatores naturais e antrópicos, que frequentemente culminam em alterações paisagísticas, como a erosão de praias arenosas. No litoral setentrional do Rio Grande do Norte (RN), a rápida expansão urbana e turística intensificou esses processos. Este estudo avalia a vulnerabilidade costeira à erosão ao longo de trechos de praias arenosas no município de São Miguel do Gostoso (RN), considerando a função protetiva de habitats naturais, especificamente dunas, vegetação e faixas de praia. A metodologia baseia-se em dados de sensoriamento remoto e

geoprocessamento, envolvendo a análise da variação histórica da linha de costa entre 1986 e 2023, por meio da aplicação do Índice de Vulnerabilidade Costeira, através do modelo *Integrated Valuation of Environmental Services and Tradeoffs* (InVEST). Os resultados indicam um aumento na mobilidade média da linha de costa no período recente (2014–2023), com intensificação das taxas mínimas e máximas de variação, especialmente em áreas sujeitas a maior antropização, onde a taxa de erosão média atinge -14,55m/ano. Constatou-se ainda que as dunas e praias arenosas funcionam como barreiras naturais eficazes, reduzindo os riscos de erosão. A conservação desses habitats é essencial para o equilíbrio ambiental da zona costeira, especialmente diante da crescente expansão urbana no município.

Palavras-chave: Infraestruturas costeiras; InVEST; Modelagem hidrossedimentar; Uso e cobertura do solo litorâneo.

1. Introduction

Coastal zones are environments of intense external geodynamics, resulting from the combined action of natural and anthropogenic factors. Hydrodynamic and climatological forcings permanently modify these environments. In parallel, anthropogenic activities and the occupation of coastal land significantly alter the spatial arrangement of natural coastal features (Chen et al., 2015). Along the coast of Northeast Brazil, this scenario of coastal landscape transformation is historical, resulting in significant changes in sediment volumes, in the physical processes of transversal and longitudinal transport, and in alterations to the biogeochemistry of coastal ecosystems (Brasil, 2002; Marroni; Asmus, 2005; Muehe, 2018; Prudêncio et al., 2019; Vousdoukas et al., 2020; Matos et al., 2022a; 2022b). Consequently, coastal communities in this region become more vulnerable to coastal dynamics, experiencing property losses and, occasionally, loss of human lives due to landslides on active coastal cliffs (Amaro et al., 2015; Pollock; Wartman, 2020; Juvino da Silva et al., 2023). Conversely, maintaining the integrity of natural habitats aids in protecting coastal zones, increasing their resilience to erosive events and, consequently, reducing environmental risks (Guannel et al., 2016).

The complex interaction between natural events and anthropogenic actions in the coastal environment frequently results in sediment erosion events on sandy beaches, characterized by shoreline retreat (Charlier; Meyer, 1998; Wannewitz et al., 2014). The shoreline is defined as the continuous linear spatial representation of the land-water interface on the beach face, which demarcates the boundary between the wet and dry beach area or the maximum inland extent of the water line from wave runup during high tide (Parker, 2003; Santos; Amaro; Souto, 2011; Amaro et al., 2015; Muehe; Klumb-Oliveira, 2014). As a readily observable natural feature, whether *in situ* or through remote sensing supported by computational algorithms, the shoreline is widely used indicator in coastal erosion studies (Luijendjijk et al., 2018; Vousdoukas et al., 2020; Almeida et al., 2021; Matos et al., 2022a).

Another approach for evaluating the erosive effects on sandy beaches is the use of vulnerability indices. Coastal vulnerability is associated with the susceptibility of natural and human systems to hazardous coastal events, including erosion, flooding, and storms (IPCC, 2014; Pollard et al. 2019). The complex relationship between forcings, the morphological response of the system, and the risk receptors requires that Integrated Coastal Management analyze erosion and flooding risks interactively (Pollard et al. 2019). From the perspective of integrated coastal management, vulnerability assessment allows for the identification of priority areas for mitigation and adaptation, supporting policies for disaster risk reduction and the conservation of ecosystem services.

Studies such as Busman, Amaro e Souza-Filho (2016) and Lacerda et al. (2022) evaluate the exposure of coastal environments on the northern coast of Rio Grande do Norte (RN) by means of physical and environmental vulnerability indices that allow for considering variables such as: geology, geomorphology, slope, pedology, vegetative cover, and land use and cover to classify the level of vulnerability. Therefore, a comprehensive analysis is required to understand the complexity of coastal vulnerability, which necessitates evaluating the influence of various variables, including anthropogenic impacts. Studies on sediment erosion and coastal vulnerability have been conducted on the RN coast (Grigio et al., 2006; Busman; Amaro; Souza-Filho, 2016; Prudêncio; Amaro; Scudelari, 2019; Amaro et al., 2021a; Matos et al., 2022a; Lacerda et al., 2022; Zamboni et al., 2022; Zamboni et al., 2025). In these surveys, coastal vulnerability assessments with and without natural coastal ecosystems revealed the importance of natural cover in protecting coastal populations against climate change and erosive processes. Furthermore, the application of geoprocessing tools has proven highly effective in coastal investigations, offering

enhanced speed, cost-efficiency, and critical consistency with ground-truthing or *in situ* observations (Almeida et al., 2021; Araújo, 2022).

This approach is particularly relevant for areas with accelerated urbanization, such as the Municipality of São Miguel do Gostoso (RN). The socioeconomic importance of this location is primarily driven by tourism, which is fostered by clear-water beaches, preserved natural ecosystems, fishing resources, and distinct landscape attributes (Brasil, 2002), in addition to activities like surfing, kitesurfing, gastronomy, and cultural events (Taveira, 2015). In this context, data from the Brazilian Institute of Geography and Statistics (IBGE, 2022) evidence that the municipality registered one of the largest demographic and economic growths in RN in the last decade. Given these factors, investigations across multiple spatio-temporal scales become essential for coastal planning and management.

This study aims to assess coastal vulnerability to erosion on the sandy beaches of São Miguel do Gostoso/RN by conducting a multitemporal shoreline analysis (1986–2023) and calculating a coastal exposure index. It also analyzes the influence of the increasing human-induced land-use change on coastal dynamics and determines the protective and mitigating role of coastal habitats, such as dunes, vegetation, and beach stretches.

2. Study Area

The area of interest encompasses a shoreline stretch within the Municipality of São Miguel do Gostoso (SMG), located on the northern coast of Rio Grande do Norte State (RN). This coastal segment was chosen due to its significant touristic appeal and the increasing process of anthropization driven by real estate and tourism sectors.

Figure 1 shows the location map of the study area, which comprises approximately 11.4 km of shoreline. Along this section, different patterns of urbanization and tourist concentration points can be observed, such as the Cardeiro, Xêpa and Tourinhos beaches, and Santo Cristo Point, and the western sector of the urban center, where new tourist developments are being implemented.

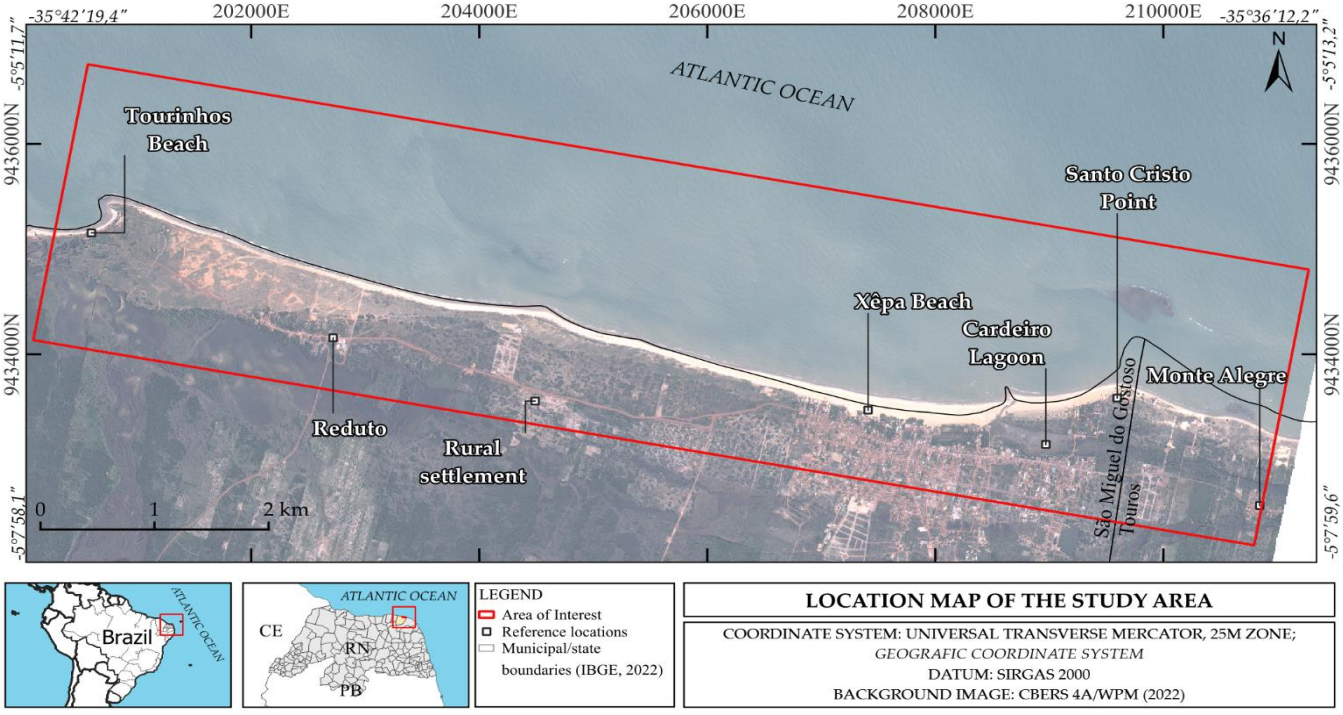

Figure 1. Location of the study area on the northern coast of Rio Grande do Norte (RN), shoreline of the Municipality of São Miguel do Gostoso.

The municipality has a northeastern tropical climate, within the semi-arid subdomain, with 7 to 8 dry months (Diniz; Pereira, 2015). The mean annual rainfall varies from 889.72 mm and 1216.17 mm, based on historical data from the TELEPLU/SMG station (EMPARN, 2022). Regarding wind incidence, the region experiences winds between 4 m/s and 7 m/s blowing from the east-southeast between December and May, and approximately 8 m/s from the predominant southeast direction between June and November (González et al., 2018).

Geologically, the area comprises two main lithostratigraphic units, according to data from the Geological Survey of Brazil (CPRM) (Pfaltzgraff; Torres, 2010): the Barreiras Group and the coastal deposits. The Barreiras Group consists predominantly of sedimentary rocks (mudstones, sandstones, and conglomerates) that form tablelands and active or inactive cliffs along the coast. Coastal deposits of beaches and mobile dunes occur in a narrow strip parallel to the shoreline and are composed of well-sorted quartz sands (CPRM, 2005, 2007).

The local geomorphology includes two relief compartments: northern coastal tablelands and coastal plains (IBGE, 2019). The coastal tablelands are flattened landforms (0–30 m in elevation) developed over sandstones and conglomerates of the Barreiras Group. In contrast, the coastal plains are Holocene formations composed mainly of marine sandy sediments (Diniz et al., 2017).

Vegetation cover within the municipality belongs to the Caatinga biome but lies near the Atlantic Forest domain, featuring steppe-savanna and pioneer formations (IBGE, 2022). The steppe-savannas, occurring inland, display typical Caatinga physiognomy with thorny shrubs and small trees (CPRM, 2005). Pioneer formations, first-occupancy vegetation on areas with marine sand deposition, are composed of herbaceous and shrub species, and may include scattered trees. Along the beachfront, these pioneer communities act as dune stabilizers (IBGE, 2012).

With a total area of 431.44 km², SMG has 5.19 km² of urbanized land, indicating an extensive portion of preserved natural areas (IBGE, 2022). The 2022 census reported a population of 10,221 inhabitants and a demographic density of 23.69 inhabitants/km² (IBGE, 2022). Historical data show pronounced population growth (the highest estimated in the state between 2018 and 2019) with a notable increase in the urban population along the coastal zone. The per capita GDP increased by 518% between 2010 and 2019, explained by intensified investments in wind energy and tourism between 2010 and 2020, corroborated by environmental licensing data from IDEMA.

Local tourism, which began in the 1990s and expanded from the 2000s onwards through the practice of nautical sports such as kitesurfing and windsurfing, has driven real estate expansion and the continuous influx of international tourists (SMG, 2025). Santo Cristo Point and Tourinhos have become prominent international tourist destinations in Rio Grande do Norte (Taveira, 2015). Santo Cristo, at the border with the municipality of Touros, stands out for its major real estate expansion, stimulated by foreign investments (Costa; Fonseca, 2019). Tourinhos Beach is mainly sought for recreational purposes, including bathing and scenic appreciation (Taveira, 2015).

3. Materials and Methods

Coastal vulnerability was assessed using the Coastal Vulnerability model from the Integrated Valuation of Environmental Services and Tradeoffs (InVEST – version 3.11.0) platform, part of the Natural Capital Project at Stanford University. Public and free databases were employed for this analysis, including the Coastal Modeling System (SMC-Brasil; Quetzalcóatl et al., 2019), the National Institute for Space Research (INPE), the Brazilian Navy, the United States Geological Survey (USGS), and the geoprocessing tool Coastal Analyst System from Space Imagery Engine (CASSIE), in addition to observational and photographic records obtained in the field for validation. This validation procedure was supported by high spatial resolution images captured by Unmanned Aerial Vehicles (UAVs or drones), which were essential for refining the classification of geological, geomorphological, and land use and land cover units, and for ensuring detailed cartographic accuracy (e.g., LOEW et al., 2017). The georeferenced data were compiled and processed using QGIS Desktop v. 3.40.5. The methodological steps of this study are summarized in Figure 2 and detailed below.

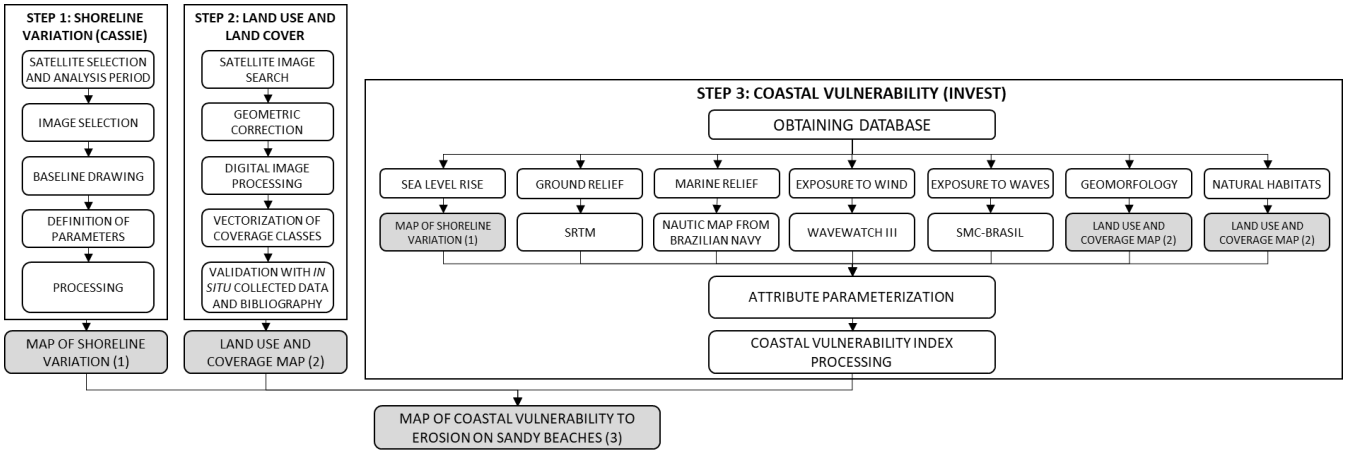

Figure 2. Methodological flowchart for shoreline variation, land use and land cover, and coastal vulnerability analysis.

3.1. Step 1: Shoreline variation

Shoreline variation was analyzed using the CASSIE tool, an open-source web platform that uses LANDSAT and SENTINEL-2 image series from Google Earth Engine. From these images, the Normalized Difference Water Index (NDWI) is generated, and through Otsu's segmentation algorithm (1979), the automatic threshold of the land-water interface is defined (Almeida et al., 2021).

Subsequently, algorithms from the Digital Shoreline Analysis System (DSAS), developed by the USGS, were used to automatically extract shorelines and calculate variation parameters. These parameters include the Shoreline Change Envelope (SCE), which quantifies the maximum distance between the most landward and seaward shoreline positions per transect; the Net Shoreline Movement (NSM), the distance (in meters) between the oldest and most recent shorelines per transect; and the Linear Regression Rate (LRR), the shoreline change rate (m/year), determined by the slope of a least squares linear regression fitted to the shoreline positions along each transect (Himmelstoss et al., 2018), which are spaced every 50 meters in this study.

Three analyses were performed using the selected satellite images: Multidecadal, referring to the unified period from 1986 to 2023; Decadal, subdividing the 1986–2023 period into four intervals of approximately 10 years each; and High-Resolution, which provides higher spatial detail than the Multidecadal and Decadal analyses, covering the period from 2017 to 2024, as described in Table 1. Only high-tide images were used (with a ±1 hour tolerance), capturing the maximum inland extent of the waterline, to minimize result oscillations.

Table 1. Analytical aspects of shoreline variation performed using the CASSIE tool.

Satellite/sensor	Spatial resolution	Analysis	Period	Number of images
LANDSAT-5/TM; LANDSAT-8/OLI	30m	Multidecadal	1986-2023	19
		Decadal	1986-1993	4
			1993-2006	3
			2006-2014	4
			2014-2023	11
SENTINEL-2/MSI	10m	High-resolution	2017-2024	10

3.2. Step 2: Mapping of geological, geomorphological, and land use and land cover features

The land use and land cover mapping supports the understanding of coastal occupation patterns by correlating natural and anthropogenic characteristics with the recorded sedimentary dynamics. For the land use and land cover map, a CBERS-4A image dated July 26, 2022, was used, with a final spatial resolution of 2 meters (after processing) and a temporal resolution of 31 days, obtained from INPE's digital catalog. The geometric correction of the image was performed using base map features from Google Earth to ensure positional accuracy and compatibility with subsequent analyses. A basic color composite image (R-3, G-2, B-1) was used for manual vectorization of cover classes, referenced by the maps of Macedo et al. (2017) and IBGE (2019) at a 1:250,000 scale. The *in situ* validation phase, a crucial step in the cartographic workflow, was executed to minimize positional

uncertainty of the mapped units and geometric misalignments that can arise from integrating small-scale cartographic databases with Remote Sensing data of varying resolutions (Noardo, 2022). Quality control, fundamental for improving the positional and thematic accuracy of the mapping (LOEW et al., 2017), was supported by drone imagery. The high spatial resolution of these images enabled a detailed verification of geological, geomorphological, and land use and land cover features in the field. The rigorous analysis and adjustment of these in situ data allowed for the production of final maps with the highest scientific detail and accuracy, providing the cartographic base for InVEST model parameterization.

3.3. Step 3: Coastal vulnerability analysis

The InVEST Coastal Vulnerability model generates an index of exposure to coastal erosion, calculated from six biogeophysical variables: relief (marine and terrestrial), natural habitats (biotic and abiotic), exposure to wind and waves, geomorphology, and sea-level change. Table 2 presents the input variables of the coastal vulnerability model, including data sources and spatial resolution.

Table 2. Input variables for the coastal vulnerability model.

Variable	Source	Scale	Spatial resolution	Temporal resolution
Relief (terrestrial)	DEM-SRTM (USGS, 2023)	-	30m	-
Relief (marine)	Vectorization of the Nautical Chart 21900 (DHN, 2022)	1:300.000	-	-
Habitats	Remote sensing using CBERS-4A images (INPE, 2022) and adaptations from Macedo et al. (2017)	-	2m	31 days
Wind	Wavewatch-III (TOLMAN, 2009)	-	55x55km grid	-
Waves	SMC-Brasil (Quetzalcóatl et al., 2019) e Wavewatch-III (Tolman, 2009)	-	55x55km grid	-
Geomorphology	Remote sensing using CBERS-4A images (INPE, 2022), adaptations from Macedo et al. (2017) and IBGE (2019)	-	2m	31 days
Sea-level change (Shoreline variation)	SENTINEL-2 (ESA, 2023)	-	10m	5 days

The relief variables refer to elevation of both land and seabed. For terrestrial relief data, the Shuttle Radar Topography Mission (SRTM) Version 4 Digital Elevation Model was used. For marine relief, bathymetric data from the Brazilian Navy's Nautical Chart 21900 were vectorized and modeled following Moura (2010). Natural habitats were defined based on the land use and land cover mapping obtained in Step 2.

For wave and wind exposure data, information from Wavewatch-III (Tolman, 2009), provided by InVEST and developed by the National Weather Service / National Oceanic and Atmospheric Administration, was used. Additionally, wave data (1948–2008) were obtained from SMC-Brasil. SMC-Brasil employs Wavewatch-III reanalysis data, calibrated and propagated by the Simulating Waves Nearshore model (Booij, Ris, and Holthuijsen, 1999), forming the Downscaled Ocean Waves (DOW) reanalysis base, which contains 60 years of reconstructed wave series between 1948 and 2008 (Camus et al., 2013). Analyzed parameters include significant wave height (Hs), peak spectral period (Tp), and mean propagation direction (Dir), as well as extreme wave events estimated using the generalized extreme value (GEV) distribution function, according to the parameterization equations below.

$$\mathrm{Hs}_{Tr} = \mu_{Hs} - (\Psi_{Hs}/\xi_{Hs}) * \left(1 - \left(\frac{1}{\mathrm{Tr}}\right)^{-\xi \mathrm{Hs}}\right) \quad (1)$$

$$Tp_{Tr} = \mu_{Tp} - (\Psi_{Tp}/\xi_{Tp}) * \left(1 - \left(\frac{1}{\mathrm{Tr}}\right)^{-\xi Tp}\right) \quad (2)$$

To characterize the offshore wave regime, the DOW point (Figure 3) was analyzed using the Mathematical and Statistical Analysis Module of Environmental Variables from SMC-Brasil. This point was chosen after comparing probability tables of Hs and Tp with points up to 21 m depth, indicating no significant deformation of

wave parameters due to bottom friction. After selecting the DOW point, the offshore wave climate for the study area was obtained, and wave propagation modeling to the shoreline was performed. Consequently, the Mean Wave Energy Flux grid was generated, and the corresponding values were extracted at Points of Interest near the study area to calculate the vulnerability index.

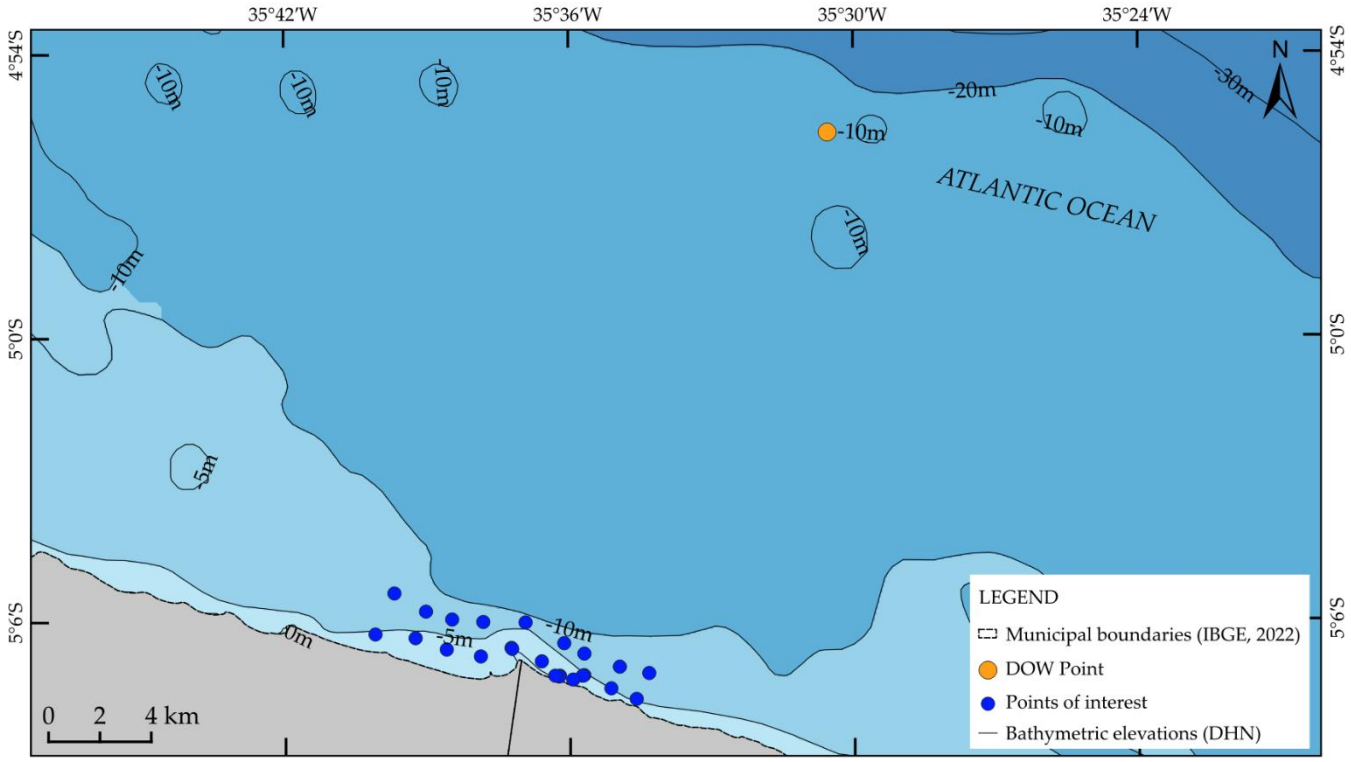

Figure 3. DOW point adopted for offshore wave climate analysis in the study area. Latitude: 4°55'41.26"S, Longitude: 35°30'32.53"W, depth: 12.18 m.

Sea-level change was assessed using the shoreline analysis results described in Step 1, subdivided into percentiles. This approach was adopted because the LRR represents a comprehensive rate considering all shoreline positions (Zamboni et al., 2022).

Each variable was assigned a score from 1 to 5, reflecting vulnerability in increasing order. This classification was established according to Table 3.

Table 3. Scoring of the input variables for the coastal vulnerability model, based on Gornitz et al. (1990), Hammar-Klose and Thieler (2001), Grigio et al. (2006), Busman, Amaro and Souza-Filho (2016), and Zamboni et al. (2022).

Variable	1-Very low	2-Low	3-Moderate	4-High	5-Very high
Relief	81 to 100 percentile	61 to 80 percentile	41 to 60 percentile	21 to 40 percentile	0 to 20 percentile
Habitats	Carnauba forest; Cliff; Dune with shrubby vegetation; Caatinga forest	Dune with herbaceous vegetation; Lagoon	Mobile dune; Agropastoral	Beach stretch; Floodplain	Anthropized area
Wind	0 to 20 percentile	21 to 40 percentile	41 to 60 percentile	61 to 80 percentile	81 to 100 percentile
Waves	0 to 20 percentile	21 to 40 percentile	41 to 60 percentile	61 to 80 percentile	81 to 100 percentile
Geomorphology	-	Cliff	-	Lagoon	Beach
Sea-level change (SLC)	0 to 20 percentile	21 to 40 percentile	41 to 60 percentile	61 to 80 percentile	81 to 100 percentile

The score of each variable served as the basis for calculating the Exposure Index (EI) to erosion, determined according to Equation 3.

$$EI = (Relief \times Habitats \times Wind\ exposure \times Wave\ exposure \times Geomorphology \times SLC)^{\frac{1}{6}} \quad (3)$$

4. Results

The results are presented in separate sections. First, the findings of the shoreline change analysis are detailed, followed by the land use and land cover mapping of the region. Finally, the results of the coastal vulnerability assessment are presented.

4.1. Shoreline variation

4.1.1.Multidecadal analysis

Figure 4 shows the result of the multidecadal analysis, and Table 4 presents the respective statistical data.

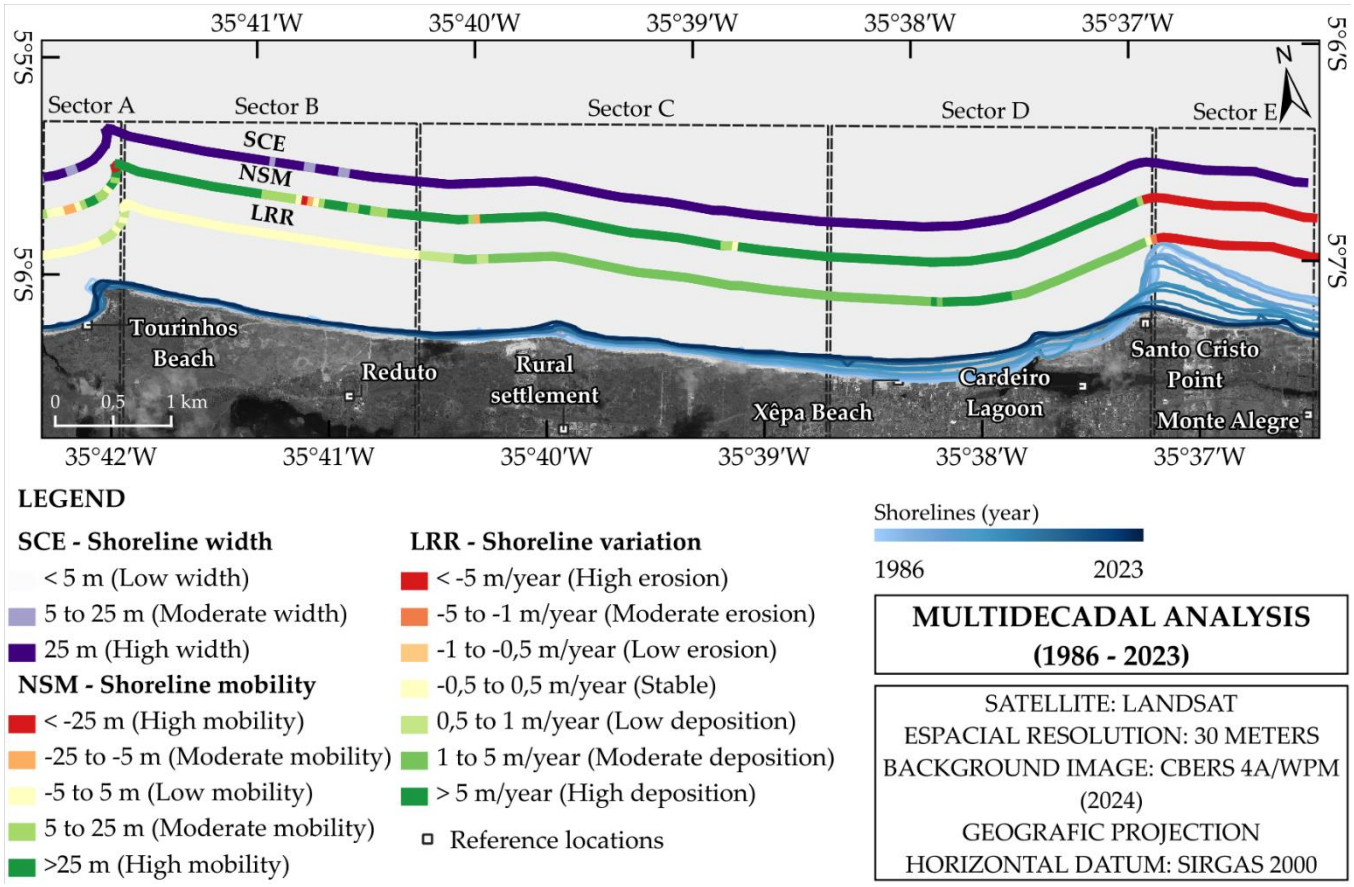

Figure 4. Multidecadal shoreline variation.

Table 4. Descriptive statistics of the multidecadal shoreline analysis between 1986 and 2023.

	Analysis parameter		
Statistic	**LRR (m/year)**	**NSM (m)**	**SCE (m)**
Mean	0,27	20,20	134,01
Median	1,19	45,90	92,04
Standard deviation	4,79	164,44	125,52
Maximum	5,55	197,24	575,91
Minimum	-16,53	-544,94	15,10
Mean - Sector A (Tourinhos Beach)	0,22	5,66	50,19
Mean - Sector B (Reduto Beach)	0,27	24,58	31,78
Mean - Sector C (Expansion zone)	1,74	69,81	83,26
Mean - Sector D (Urban beaches)	4,07	151,64	176,87
Mean - Sector E (Santo Cristo Point)	-11,39	-378,43	419,47

The shoreline mapping shows changes in the coastal shape during the analyzed period, especially at Santo Cristo Point, with an average linear retreat of -378.43 m and an amplitude of 419.47 m. This altered the regional beach morphology and reduced the shoreline by about 600 m. At the Tourinhos Beach promontory, shoreline changes are more subtle.

The shoreline change rate (LRR) (1986–2023) shows an overall stable profile with a trend toward deposition (0.27 m/year) in 29% of the sector. At Santo Cristo Point, the greatest variation occurs, with an average erosion of -11.39 m/year along a segment of approximately 1.4 km, and average deposition of 4.07 m/year along 6.4 km of adjacent leeward urban beaches. These results indicate sediment flux from east to west, originating from Santo Cristo Point and deposited along the urban beaches of Cardeiro and Xêpa, straightening the shoreline toward an overall east-west orientation. The original shoreline configuration at the site had a "zeta" (ζ) shape, which in plan view is asymmetric, showing a decreasing curvature radius toward one end (Chapman, 1984). This previous morphology was altered by erosive processes that caused longshore sediment transport to the west and the consequent infilling of the embayment with material eroded from Santo Cristo Point, resulting in the current straighter shoreline. Such a change in shoreline planform morphology, where Santo Cristo Point acts as a diffraction point, increases beach exposure to wave action. In the western sectors beyond the urban limits, the pattern ranges from moderate deposition in the expansion zone (average LRR of 1.74 m/year) to stability at Reduto and Tourinhos beaches, whose average shoreline variation is 0.27 and 0.22 m/year, respectively.

Regarding shoreline mobility (NSM), most of the coast (71%), about 8.15 km, shows high mobility, indicating intense sediment dynamics from Santo Cristo Point to the rural settlement shoreline. Beyond this section, mobility remains low to moderate. The amplitude of shoreline variation (SCE) is high throughout most of the study area, oscillating to moderate levels in the western portion.

4.1.2.Decadal analysis

Figure 5 illustrates the map of decadal shoreline variation, covering the period from 1986 to 2023. This analysis was subdivided into four distinct periods. Table 5 presents the statistical results of the variables for each period.

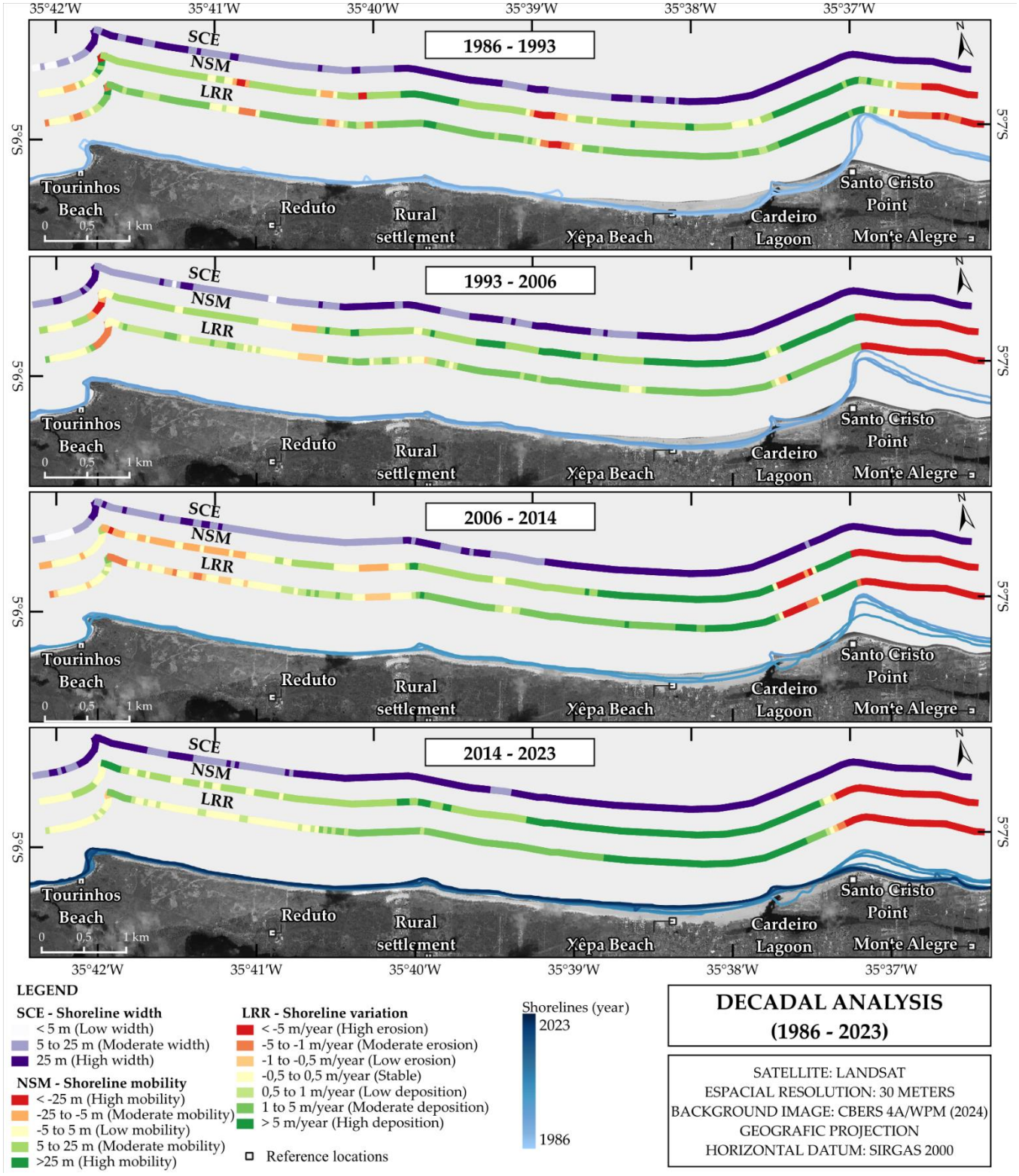

Figure 5. Analysis of the decadal shoreline variation.

Table 5. Descriptive statistics of shoreline variation for the transects analyzed over four decades, from 1986 to 2023.

Analysis parameter	Statistic	Period			
		1986 to 1993	1993 to 2006	2006 to 2014	2014 to 2023
LRR (m/ano)	Minimum	-7,46	-9,70	-26,95	-26,55
	Mean	1,76	0,11	-0,75	0,25
	Maximum	35,01	5,56	7,96	14,52
NSM (m)	Minimum	-87,39	-123,82	-217,98	-235,99
	Mean	13,44	4,81	-8,49	9,90
	Maximum	228,79	88,97	63,60	228,21
SCE (m)	Minimum	0,00	2,17	0,00	12,23
	Mean	33,74	37,04	43,22	64,40
	Maximum	235,55	166,91	217,98	235,99

The shoreline change rate (LRR) indicates that the first period (1986-1993) was the only one with an average depositional pattern, with a mean erosion rate of 1.76 m/year. The third period (2006 to 2014) was the only one with an average erosive pattern (-0.75 m/year), while the other periods indicate an average stable pattern. At Santo Cristo Point, the erosive intensity accelerated over the decades: -1.68 m/year between 1986 and 1993, -7.98 m/year between 1993 and 2006, -15.48 m/year between 2006 and 2014, and -17.66 m/year between 2017 and 2023.

The shoreline mobility (NSM) is similar across the four decades, with a predominance of moderate and high mobility sectors. The mean magnitude of shoreline change (SCE) was higher in the more recent decades, due to the intensification in the eastern sectors. The greatest suppression of the beach berm at Santo Cristo Point occurred in the most recent periods from 2006 to 2023, ratified by the high SCE value in that period.

4.1.3. High-resolution analysis

Figure 6 illustrates the results derived from the analysis of remote sensing images from the SENTINEL-2 satellite in the period between 2017 and 2024. Table 6 complements this, detailing the statistical analysis.

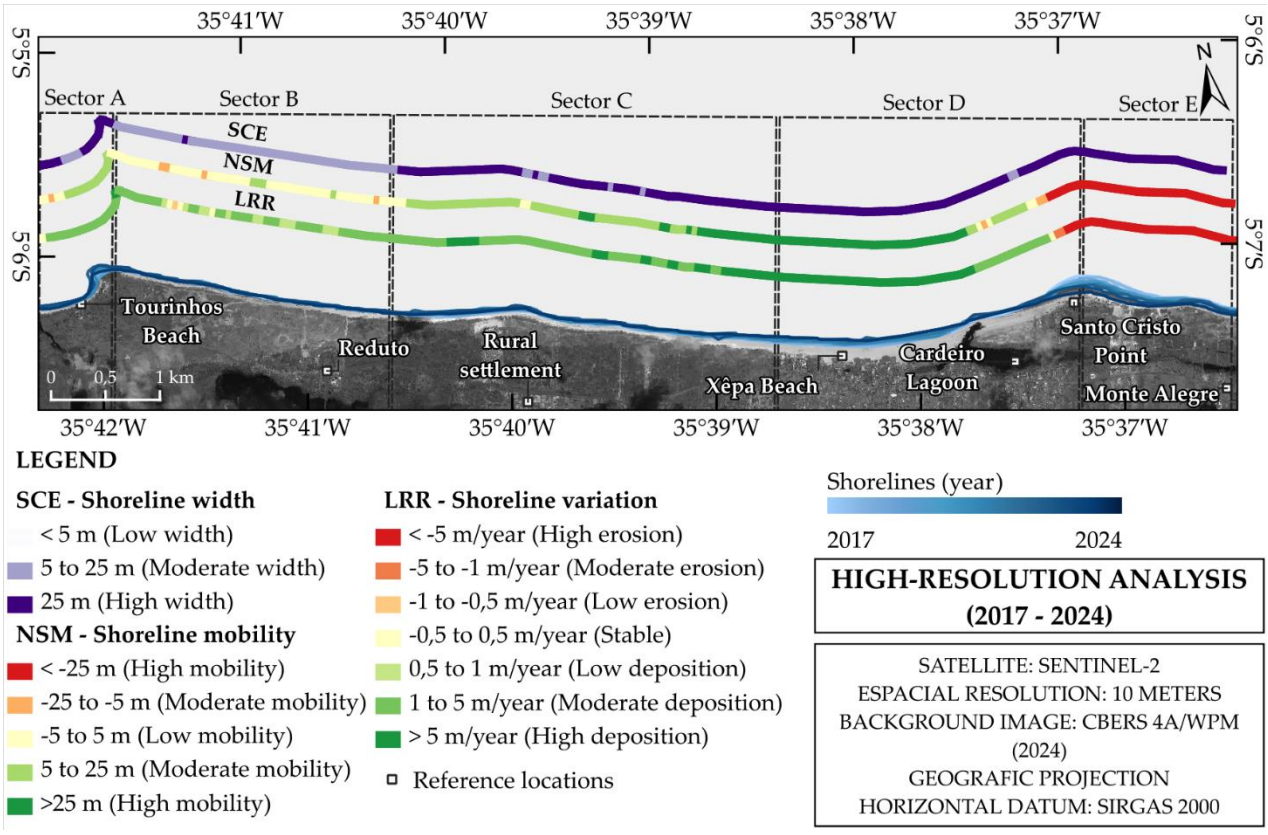

Figure 6. Variation of the shoreline in the high-resolution analysis.

Table 6. Descriptive statistics of the high-resolution shoreline analysis between 2017 and 2024.

Statistic	Analysis parameter		
	LRR (m/ano)	NSM (m)	SCE (m)
Mean	1,81	1,19	44,80
Median	2,81	7,89	35,58
Standard deviation	7,75	48,62	31,81
Maximum	12,21	62,16	162,37
Minimum	-24,29	-162,37	9,60
Mean - Sector A (Tourinhos Beach)	3,35	5,57	38,95
Mean - Sector B (Reduto Beach)	1,20	-0,08	17,11
Mean - Sector C (Expansion zone)	4,63	19,57	36,60
Mean - Sector D (Urban beaches)	6,26	26,83	55,14
Mean - Sector E (Santo Cristo Point)	-14,55	-99,62	99,65

The coastal dynamics observed in the 2017 to 2024 period corroborates the multidecadal spatial pattern previously identified. However, this new analysis reveals a notable intensification of sediment deposition, especially at Xêpa Beach, with deposition rates on the order of 6.26 m/year, in contrast to the very high erosion rates of -14.55 m/year recorded at Santo Cristo Point. In the other sectors to the west of the study area, a low-intensity average depositional pattern predominates, with mean LRR values between 1.20 and 3.35 m/year, associated with moderate mobility.

The high-resolution and multidecadal analyses converge in the spatial indication of shoreline mobility. The intensity of the erosion-deposition processes is more pronounced in the eastern portion of the study area, correlating with the most anthropized region, especially near the urban center of SMG.

4.2. Land use and land cover

Figure 7 presents the land use and land cover map, the result of the analysis and interpretation of the CBERS-4A multispectral image from 06/22/2022. The validation of the mapping occurred through field surveys, complemented by photographic records that exemplify each of the 11 classes identified in the study area.

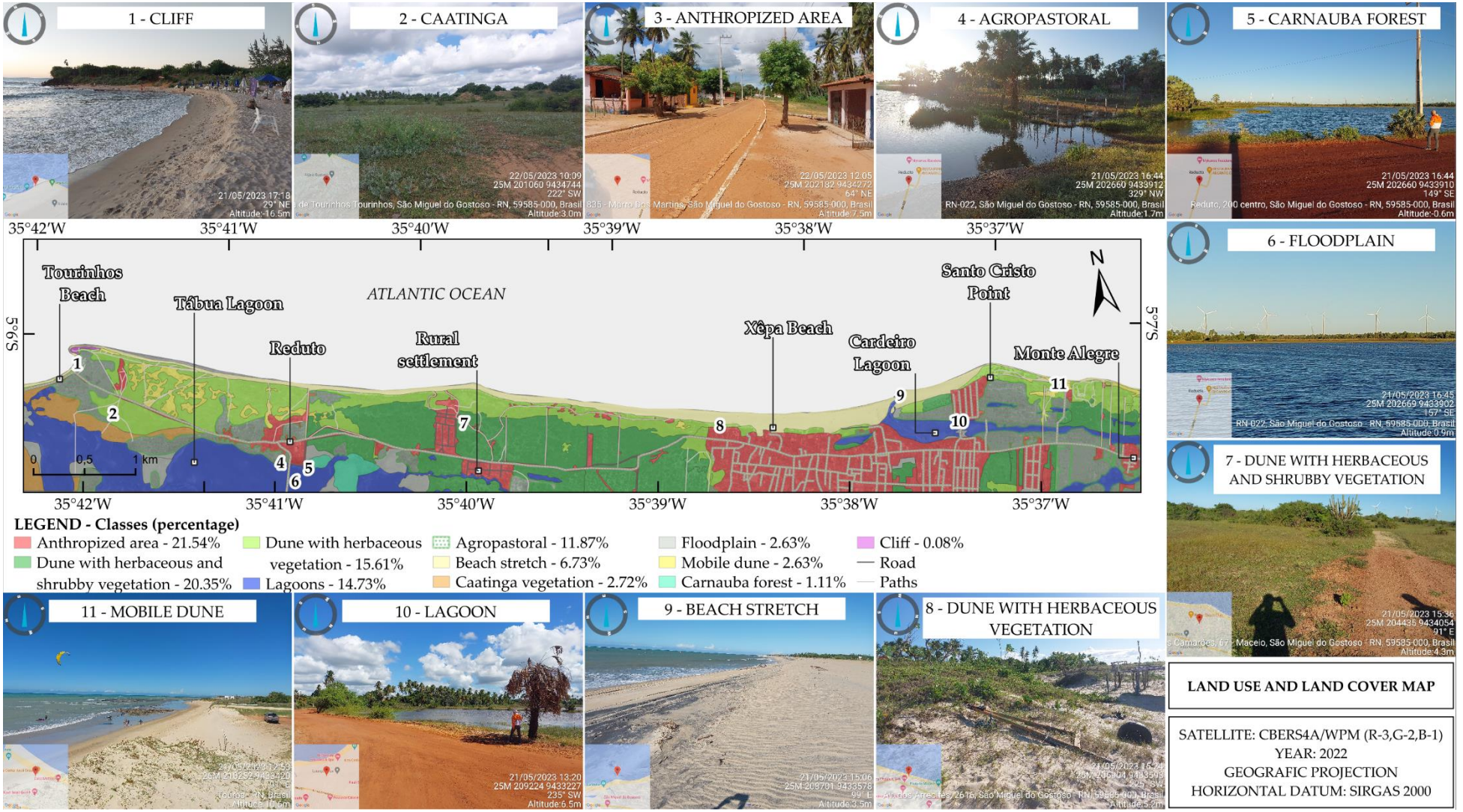

Figure 7. Land use and land cover map with field records in the study area, exemplifying the identified classes.

Cliffs occurred only at Tourinhos Beach, where steep sedimentary rocks under continuous erosion were observed. Field surveys confirmed this site as a point of anthropogenic interest, with frequent tourist visits for landscape contemplation.

To the south of Tourinhos Beach, in an area adjacent to Tábua Lagoon, a hypoxerophilous caatinga physiognomy was identified. This vegetative formation is characteristic of Coastal Plateau environments established on a pedological substrate of predominantly Red-Yellow Latosol nature. The darker coloration observed in the surface horizon (A horizon) is intrinsically connected to the increase in organic matter content, favored by the hydromorphic condition localized by the proximity to the lagoon area, resulting in slower decomposition processes under greater water saturation (Macedo et al., 2017). On the margins of Tábua Lagoon, a carnauba forest (*Copernicia prunifera*) was noted, alternating with agricultural activities.

The mapped anthropized areas include the Reduto community, the urban center of SMG, and the rural settlement, strategically located between these nuclei. Roads and vehicle trails, discernible in satellite images, were also categorized as anthropized areas. The agricultural class predominantly covers the cultivation of coconut trees, in addition to other smaller-scale crops and animal husbandry. This type of land use is more pronounced near Tábua Lagoon and in the eastern portion of the municipal center of SMG.

Floodplains were identified in areas adjacent to water bodies, especially near Tábua Lagoon. In these locations, the terrain exhibits moisture and signs of salinity, suggesting saline intrusion. Natural and anthropogenic vegetative cover is insignificant in these fields. Along the shoreline, dune fields with distinct typologies of vegetative cover were delimited. Immediately after the beach stretch, which extends along the entire coast, dunes with herbaceous vegetation were identified.

Further beachfront, in the central portion of the coast, a transition to dune fields with shrubby vegetation is observed. In areas of greater anthropogenic density, extensive dunes devoid of vegetation were recorded.

The mapped lagoons are the Cardeiro and Tábua, with diffuse spatial configurations for their beds. During the field survey, these temporary lagoons exhibited a water level.

The mapping revealed the predominance of anthropized areas, which constitute 21.54% of the study area. Next in prominence are the dunes with herbaceous and shrubby vegetation (20.35%) and the dunes with herbaceous vegetation (15.61%). The study area maintains significant vegetative cover, especially in the dune fields. However, the data also evidence the expansion of anthropogenic occupation.

4.3. Offshore wave climate

At the DOW point (1948-2008), the predominant waves come from North and East-Southeast: 39.40% from East; 22.74% from East-Northeast; 17.15% from Northeast; 10.39% from North-Northeast, and 1.39% from North (Figure 8). Probabilities of 8.84% and 0.08% were obtained for waves from East-Southeast and Southeast, respectively. However, these wave fronts reaching the DOW point do not significantly affect the shoreline in the area of interest, being almost parallel to it.

The mean Hs (or with 50% probability of non-exceedance - Hs50) is 1.40 m from East and 1.45 m from East-Northeast, which represent 62.14% of the probability of occurrences. The Hs50 from Northeast is 1.57 m; mean waves with 1.80 m come from North-Northeast, representing 27.54% of the wave regime. Mean waves coming from North have 2.22 m Hs, with 1.39% probability of occurrence.

During sea storms, the wave exceeded 12 hours per year (Hs12) is between 2.13 and 2.46 m coming from East and Northeast, representing 79.29% of the probability of this occurrence at the DOW point. Waves from North-Northeast and North presented Hs12 of 3.86 and 4.07 m, respectively, summing up to 11.78% of the regime probability. Despite lower occurrence, these significant wave height values are considered severe for the region, and are warned as high risk for navigation by the Brazilian Navy's Notice to Mariners Bulletin. These waves reach the shallower portions of the continental shelf with high hydraulic energy for sediment mobilization, commonly related to the most intense episodes of sand removal from the swash zone at the shoreline, during storm events. That is, on a scale of hours, the sediment removed from the swash zone is carried to the nearshore compartment, where it is liable to be transported out of the beach geodynamic system by longshore drift currents.

The joint density function Hs-Tp indicates that most occurrences were concentrated in waves with 1.5 m Hs and Tp of approximately 8.6 s (Figure 8b), suggesting a mean wave regime generated by local winds, near the DOW point.

The multivariate analysis of wave parameters indicated that waves with Hs > 2.4 m (red tones in Figure 8c) have Tp greater than 13 s (darker green tones in Figure 8c), associated with North-Northeast directions (arrows in Figure 8c). This data indicates that waves with the highest potential for sediment mobilization, occurring during storms, form in locations distant from the study area and propagate to the DOW Point. Since deep-water wave groups tend to become parallel to the wind field that generated them, the directions point to a predominance of northeastern trade winds.

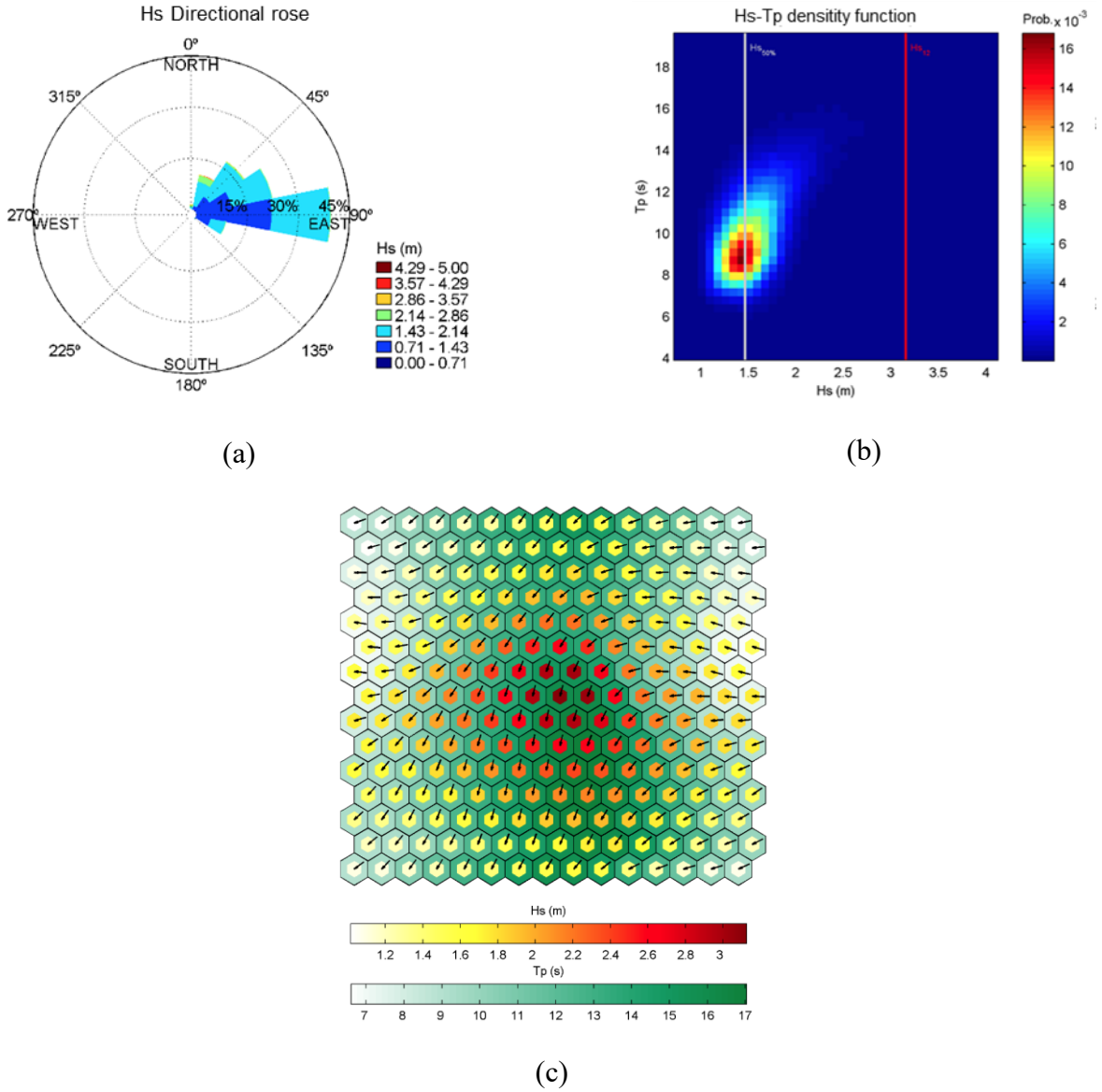

Figure 8. Graphs of the offshore wave climate evaluated at the DOW point. (a) Directional rose diagram of wave occurrence probabilities for Hs values. (b) Hs-Tp joint density function. (c) Multivariate characterization of wave parameters. Cores in shades of white, yellow, orange, and red indicate Hs values; the borders, in shades of white and green, indicate Tp values; internal arrows indicate the Direction

Seasonally, North-Northeast and Northeast waves reach the area during the months of December to May, summer and autumn conditions in the study area (Figure 9a,b), months in which the Intertropical Convergence Zone (ITCZ) is acting in its southernmost climatological position (Souza; Cavalcanti, 2009; Melo; Cavalcante; Souza, 2009). In this way, the northeastern branch of the trade winds acts in the region of the DOW point. East waves begin to appear during the months of March to May and predominate from June to November (Figure 9c,d). During the winter and spring months, the southeastern branch acts over the region, aided by upper-level cyclonic vortices over the Brazilian Northeast coast and by the approximation of the South Atlantic High Pressure System to the Brazilian east coast (Reboita; Ambrizzi; Da Rocha, 2012). In drier years or with positive sea surface

temperature anomalies in the North Atlantic, the ITCZ acts displaced to the north of its climatological position (Souza; Cavalcanti, 2009), favoring the action of the southeastern branch of the trade winds in the study area starting in April and May (Figure 9b).

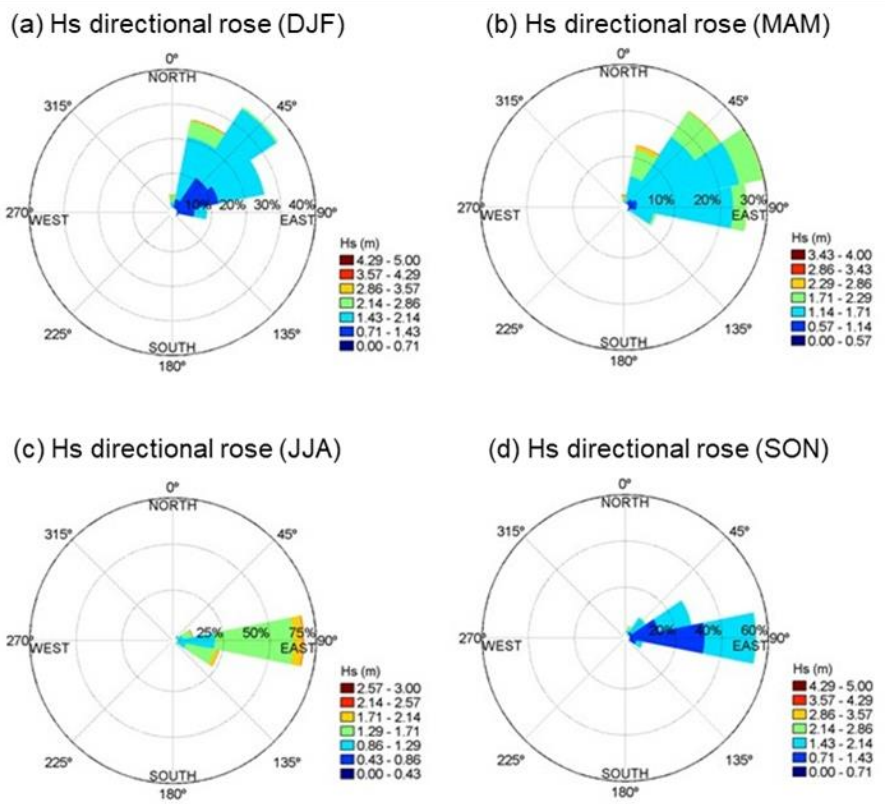

Figure 9. Seasonal Hs diagrams at the DOW point ; for the months of (a) December, January, and February - DJF; (b) March, April, and May - MAM; (c) June, July, and August - JJA; (d) September, October, and November - SON.

The GEV parameterized equation for Hs and Tp indicates that the wave with a return period Tr of 60 years has 4.20 m and 19.81 s, at a 5% confidence level (Figure 10a,b).

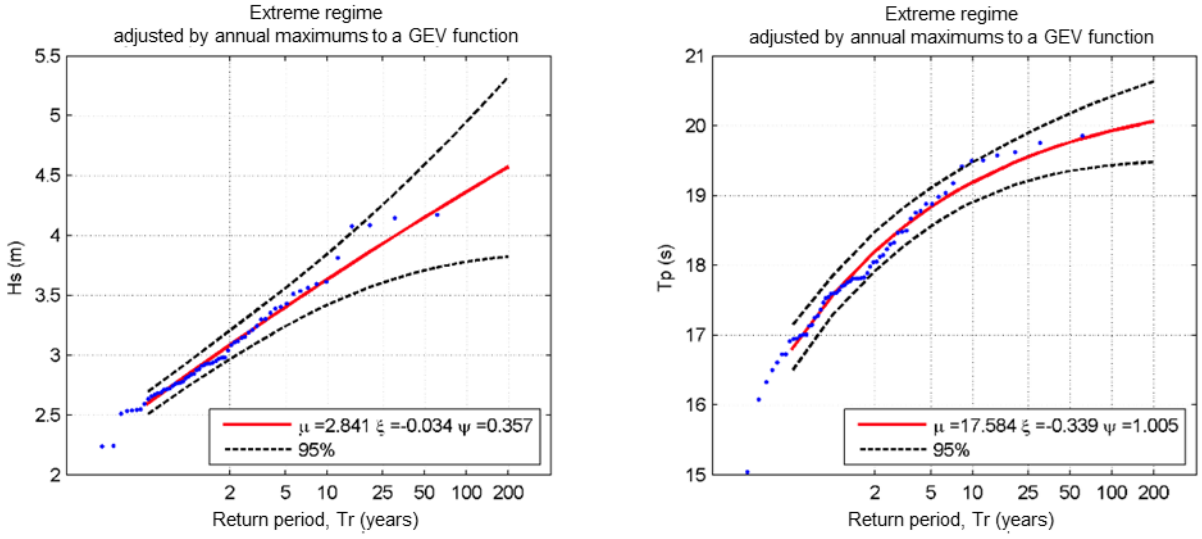

(a) (b)

Figure 10. Generalized extreme value adjustment of (a) Hs and (b) Tp, at the DOW point.

The annual maximums of Hs and Tp (Figure 11) confirm that storm waves, with higher Hs values (>2.4 m), present Tp > 10 s, being generated in source areas distant from the DOW point and influenced by large-scale tropical atmospheric events in the Atlantic Ocean.

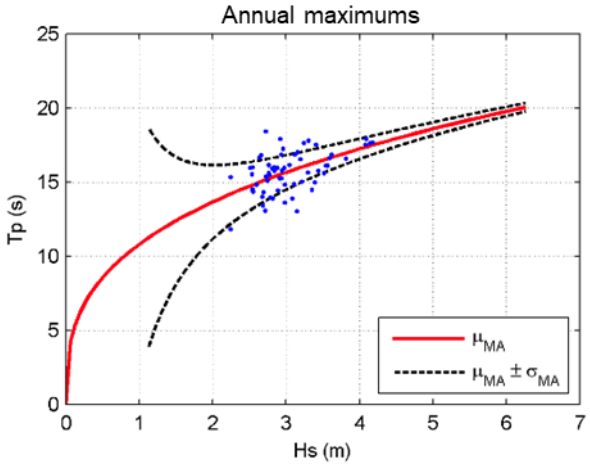

Figure 11. Graph of the annual maximums of Hs and Tp at the DOW point.

4.4. Tide regime

The data series for the DOW point had the tide levels modeled from tide gauge data from the Brazilian Navy's Directorate of Hydrography and Navigation, referenced to the local mean sea level at the Guamaré Port tide gauge.

The astronomical tide in the study area is semi-diurnal under a mesotidal regime, with high and low tide cycles approximately every 6 hours, and a total mean amplitude of 2.84 m (Figure 1). The contribution of the meteorological tide shows a modular variation of ±0.09 m relative to the mean sea level (Figure 12b).

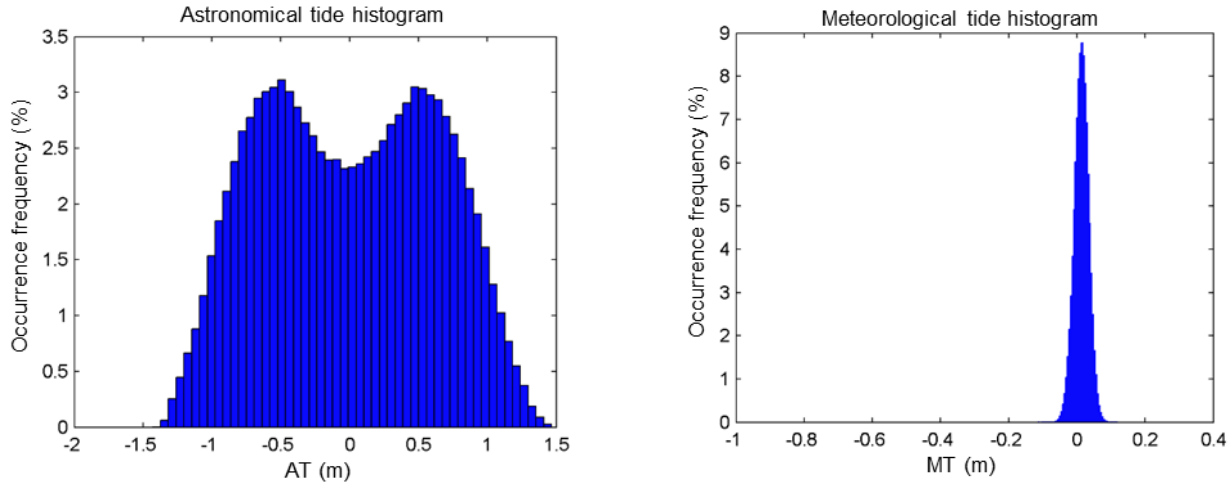

Figure 12. Histograms of (a) astronomical tide and (b) meteorological tide at the DOW point.

4.5. Coastal vulnerability

Figure 13a presents the results of coastal exposure to erosion imposed by each variable considered in the analysis: waves, winds, sea-level change, relief, geomorphology, and land use and land cover. Figure 13b, in turn, presents the coastal vulnerability index of the study area, detailing the exposure with and without considering the protective function of the habitats.

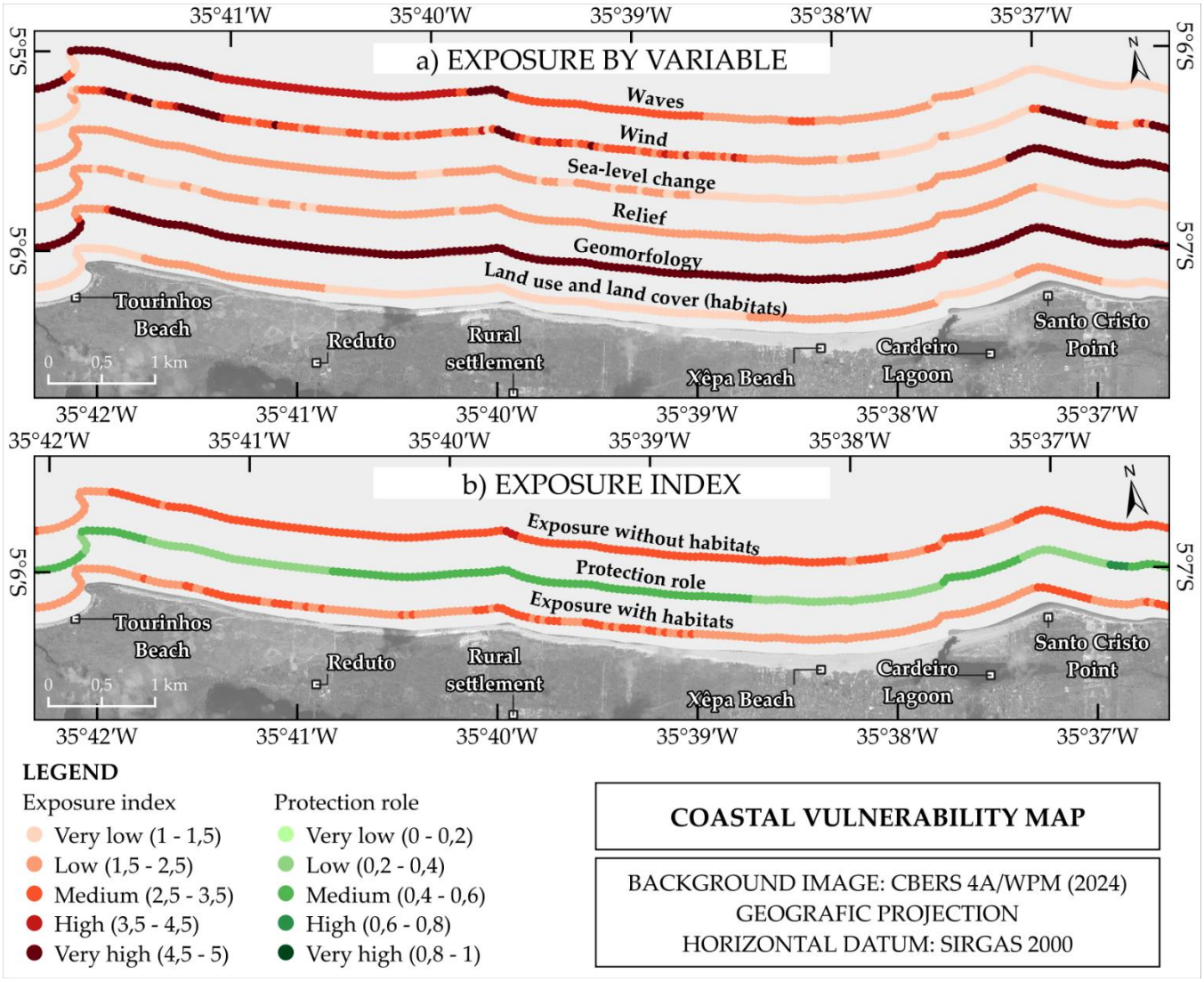

Figure 13. Coastal vulnerability exposing: a) the level of exposure associated with each of the variables considered in the final index. b) the erosion exposure indices along the studied coast considering the protection resulting from the habitats (in green) and without the protection of the habitats.

Figure 13b reveals that the presence of coastal habitats is crucial for mitigating exposure to erosion, keeping it at low to medium levels. In contrast, the absence of this protection results in a predominant elevation of vulnerability to the medium index, with the emergence of a high-vulnerability sector north of the rural settlement, in the central portion of the study area. Beach geomorphology, predominantly sandy, is a primary factor of susceptibility to erosion, as evidenced in Figure 13a. Additionally, the vulnerability associated with wave and wind action demonstrates a significant impact on this environment, particularly where the morphology of the sandy beach forms almost orthogonal angles to their incidence.

The mean sea-level change, inferred by the planimetric variation of the shoreline (i.e., the erosion rates at points along the coast), exerted a notable impact, particularly near Santo Cristo Point. In the western sector, notably at Tourinhos Beach, waves also proved to be a significant factor in coastal vulnerability. The relief and land use/occupation contributed to the general modulation of vulnerability in the study area. Statistical analysis revealed that the median exposure index, considering the protection of coastal habitats, was 2.39±0.27 (low risk). However, without this protection, the median rose to 2.80±0.29 (medium risk), emphasizing the importance of the ecosystem services of protection against coastal erosion and flooding provided by these environments. The scatter plots of coastal vulnerability values are presented in Figure 14.

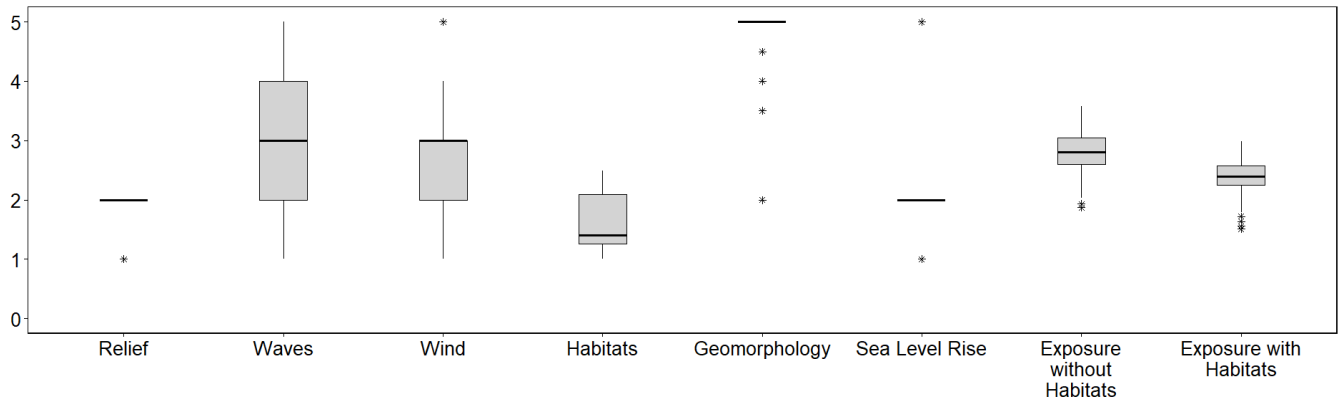

Figure 14. Box-plot diagram of the scatter of coastal vulnerability exposure data.

Figure 14 demonstrates that the presence of habitats is associated with a significant reduction in exposure to coastal erosion in the study area, evidenced by the distinction in the data groupings. Additionally, the results make explicit greater heterogeneity in the distributions of the variables waves, wind, and land use and occupation compared to relief, geomorphology, and sea-level change.

The outliers identified reflect specific local conditions or punctual features that deviate from the predominant pattern, possibly associated with the spatial heterogeneity of certain stretches of the study area. As an example, for geomorphology, considering that the shoreline is mostly beach, the other features (lagoons and cliffs) were defined as outliers. The outlying values in the exposure indices without and with habitats reflect small stretches of lower exposure in the study area.

5. Discussion

The analysis of shoreline variation in the study area, from 1986 to 2023, revealed spatially heterogeneous variation rates. Notably, approximately 1.4 km of the coast exhibited erosion rates greater than 5 m/year, a magnitude classified as extreme erosion in a global perspective, as demonstrated by comparable studies in similar periods (Luijendijk et al., 2018). At Santo Cristo Point, a mean linear continental retreat of -378.43 m was observed between 1986 and 2023 (reaching a maximum value of 575.91 m), with erosion rates on the order of -11.00 m/year, corresponding to a planimetric area loss of about 585,036 m², as detailed in Figure 15. In the higher-resolution analysis, with data from a more recent period (2016 to 2024), the erosive trend intensifies, reaching a mean value of -14.55 m/year. These results unequivocally evidence the severity of the erosional processes in the region, particularly at points of high vulnerability.

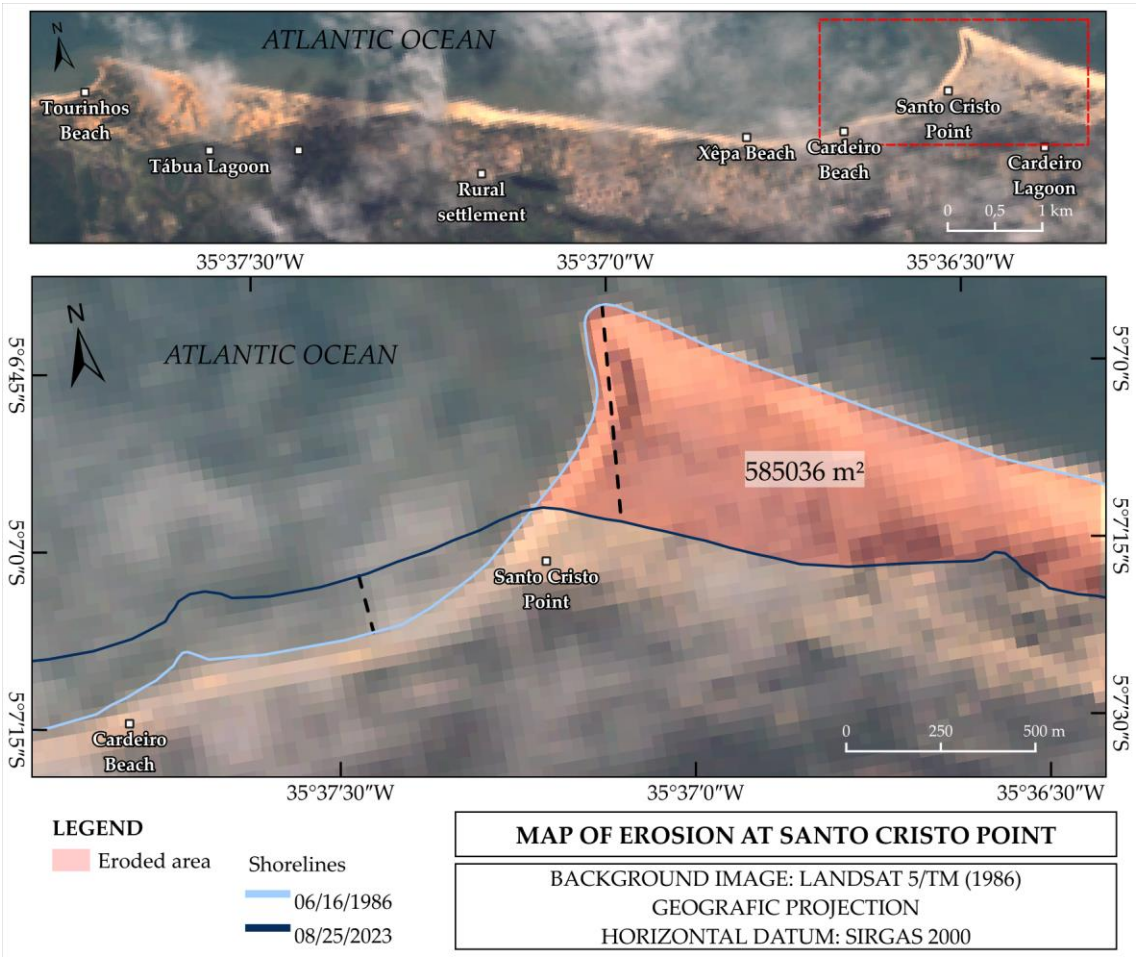

Figure 15. Eroded area at Santo Cristo Point between the years 1986 and 2023.

The intensification of sedimentary dynamics in the study area in recent decades was observed, evidenced by the accentuation of the variation rates (LRR) and magnitude of variation (SCE). Extreme erosion, greater than 5 m/year, was recorded along 11% of the coast between 1986 and 1993, 14% between 2006 and 2014, and 21% between 2014 and 2023, demonstrating a progressive increase in the extent of areas with severe erosion. Regarding the magnitude of change (SCE), the high magnitude classification, above 30 m, was observed along 61% of the evaluated stretch between 1986 and 2006, 56% between 2006 and 2014, and a notable increase to 83% in the most recent decade (2014 to 2023), emphasizing the amplification of shoreline instability over time. This data confirms a scenario of worsening coastal erosion in the region, with significant implications for coastal management and territorial planning. This situation is exacerbated by meteo-oceanographic pressures arising from extreme events with decadal return periods, whose frequency is intensified by climate change due to global warming. The DOW data evidences the influence of tropical atmospheric phenomena on the waves incident on the study area, carrying potential energy for the hydraulic mobilization of sediments on the beach. Despite being short in time, lasting only a few hours, intense meteo-oceanographic events are directly related to coastal disasters with great environmental impact (Pinheiro et al., 2023).

Changes in shoreline dynamics are prominent in the eastern sectors of the study area, adjacent to Santo Cristo Point, and the central beaches of Xêpa and Cardeiro. In these areas, the variation rates exhibit noticeable modification starting from 1993–2006. It is crucial to note that the acceleration of erosive processes observed in the study area coincides with the urban development of SMG. This development intensified starting in the 2000s, characterized by the intensification of beach use, installation of tourist infrastructure close to the seafront, increase in floating population, practice of nautical sports, and changes in social dynamics (Matias, 2017). Such results suggest a strong correlation between anthropogenic pressure and the worsening of coastal erosion in the region.

It was found that the coastal segments with the most intense variation rates (erosion or deposition greater than 5 m/year) are located in the vicinity of more consolidated urban areas. In contrast, in the sector with a lower

degree of anthropization, situated between the urban center of SMG and Tourinhos Beach, a more stable profile is noted, with small oscillations throughout the analysis period. These results indicate a direct correlation between human occupation and coastal dynamics, suggesting that anthropization induces an imbalance in the sedimentary budget, mainly due to the interruption of sediment supply from the continent, resulting from soil impermeabilization due to the construction of buildings near the shoreline (Figure 7). In these sectors with the most preserved beach features, despite the incidence of storm waves and intense sea agitation, the beach still performs the ecosystem function of coastal protection, capable of restraining the sea's advance and acting as an adaptive regulator against medium- and long-term climatic pressures. This relationship is consistently corroborated by several other studies (Addo; Jayson Quashigah; Kufogbe, 2011; Hennig, 2016; Forgiarini et al., 2019; Daud; Milow; Zakaria, 2021).

The vulnerability analysis at Tourinhos Beach revealed a consistently low index in both scenarios (with and without coastal habitats). This condition is primarily attributed to the likely lower impact of wave energy locally, in addition to the sandy strip being reduced or nonexistent at low tide, directly in front of the active cliff. The presence of this active cliff confers lower vulnerability to erosion compared to shoreline analyses in sandy stretches. Such results highlight the importance of the stability of coastal geomorphology in modulating vulnerability, even in the face of environmental changes.

From Tourinhos Beach to Xêpa Beach, a stretch of the beachfront with emerging tourist and real estate interest, oscillation between medium and low risk is observed. This variation is predominantly influenced by vulnerability to waves when the presence of habitats is considered. However, when disregarding the protection of these ecosystems, the risk rises to the medium level in almost the entire sector, with the identification of approximately 150 m highly exposed to erosion.

At Santo Cristo Point, high vulnerability was associated with factors such as wind, geomorphology, and planimetric variation of the shoreline (sea-level change), with mild exposure to waves. This is possibly attributed to the nearby submerged rocky structure, which refracts and diffracts the wave climate, reducing the Wave Energy Flux (FE) of the waves that reach the local coast. Consequently, the vulnerability index for this sector was classified as medium, regardless of the presence of habitats.

The mapping of land use and land cover, together with *in situ* recognition, revealed that, in areas with greater human presence, the dune fields, which act as natural barriers against hydrodynamic forcings, are attenuated and frequently devoid of significant vegetation. Such a factor results in a more energetic coastal system and, consequently, one more susceptible to sediment loss due to oceanic and coastal movement. The impact of anthropization is not restricted to fixed occupations near the coast, but is accentuated by the increased flow of passers-by, bathers, and vehicles. This typically concentrates near inadequately constructed structures on the coast, impacting dunes and beach stretches, as per *in situ* recognition.

The coastal vulnerability analysis ratifies the importance of dune fields and back-beach dunes, especially in the sector extending from Xêpa Beach to Tourinhos Beach. This region demonstrated a significant reduction in exposure to coastal risks, but is subject to increasing real estate and tourist interests, with new developments being installed or planned. It was verified that the presence of preserved dune fields mitigates vulnerability along approximately 2.6 km of the beachfront (Figure 16). Furthermore, the wide beach strip between Santo Cristo Point and Xêpa Beach also plays a relevant protective role, although the dune-beach system in this segment has been compromised by inadequate anthropization.

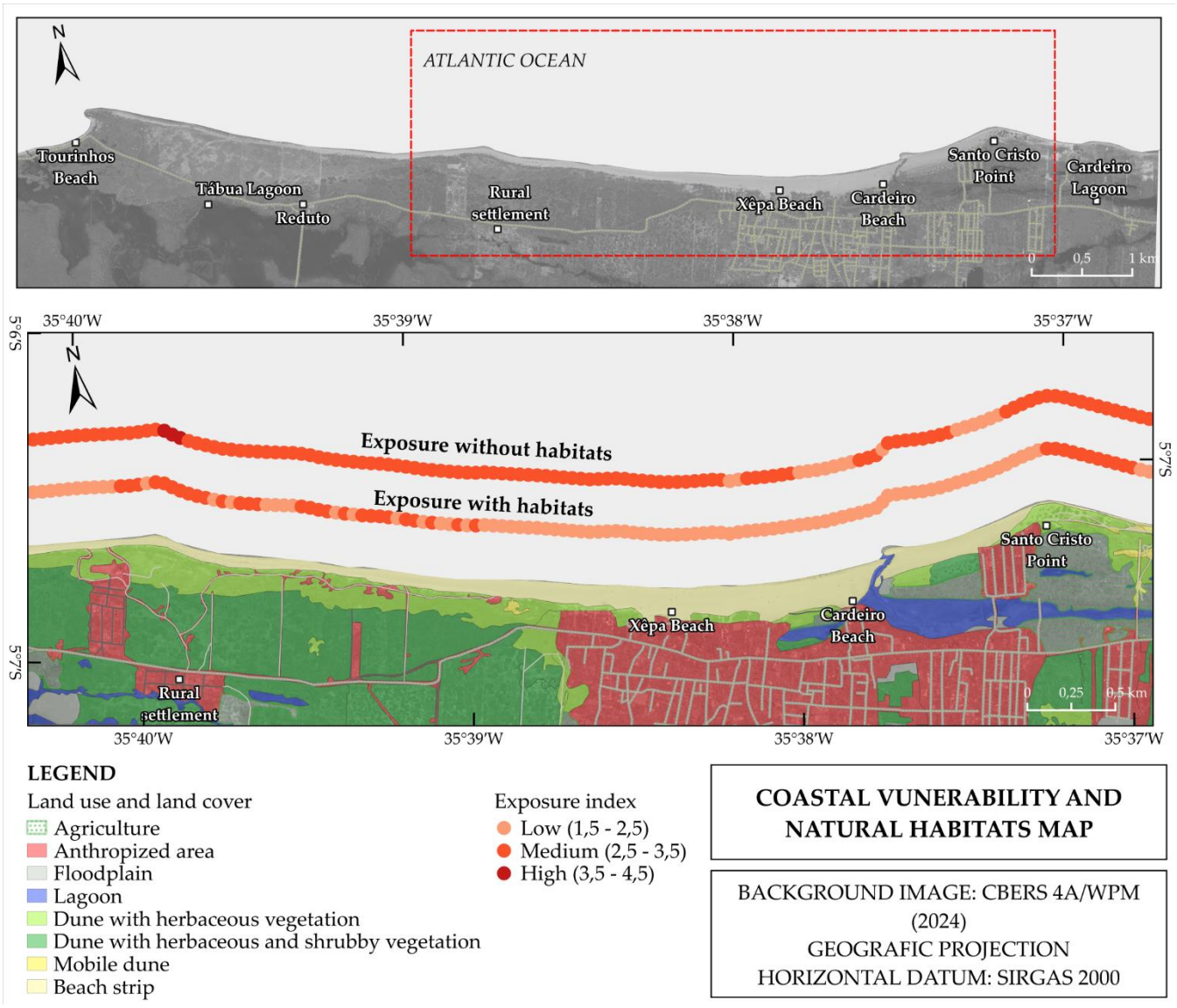

Figure 16. Vulnerability map of the urban sector with an overlay of the mapped land use and land cover, evidencing the protection resulting from the present coastal habitats.

The results of the coastal vulnerability assessment evidence the multifactorial and interrelated nature of the processes that govern the exposure of the shoreline to hydrodynamic forcings, anthropogenic activities, and the consequent erosional and depositional effects. For the study area, the crucial variables in determining coastal risk include: the morphology of the coast, given its direct relationship with exposure to wind incidence and marine action; the proximity of coastal habitats, such as the presence of adjacent dunes and the extent of the beach stretch; and the mean sea-level change. Consequently, the alteration of the shoreline, driven by shoreline variation and accelerated by the removal of protective habitats, may imply the intensification of coastal dynamics, resulting in a cumulative effect of adverse impacts on the coastal area, which presents increasing socioeconomic interest.

The locations with the highest exposure to erosive effects in the studied area were Santo Cristo Point and the municipality's urban beaches (Cardeiro and Xêpa), characterized by significant tourist investments, as evidenced by the new developments. Indiscriminate anthropogenic occupation, concomitant with the suppression of protective habitats against erosion, may result in severe consequences for local tourism. This will manifest through the reduction of the beach strip, the deterioration of coastal water quality, loss of green spaces, and, in more extreme scenarios, the loss of public and private property, coastal equipment and infrastructure, a phenomenon already occurring in the area.

6. Conclusions

This study evaluated the coastal vulnerability of a beachfront segment in São Miguel do Gostoso, RN, focusing on its relationship with the increasing intensification of hydrodynamic energy and the process of inadequate anthropogenic land use. The methodology employed geoprocessing techniques that coupled orbital remote sensing data, numerical coastal and oceanic modeling, and field surveys, providing a robust spatial and temporal analysis.

The results revealed extreme erosion rates, reaching an average of -14.55 m/year in a sector of the study area's sedimentary budget, a magnitude classified as severe in a global context. Furthermore, the period from 1986 to 2023 demonstrated significant variations in the sedimentary balance profile, with a notable accentuation of sediment mobility and in the shoreline change rate starting from 2004, and more expressively after 2014. This intensification was prominent in locations of higher density of anthropogenic occupation, such as Santo Cristo Point and the beaches of Cardeiro and Xêpa.

The mapping of land use and land cover, allied with *in situ* recognition, confirmed the anthropization process of the area, although significant natural cover still persists. The dune features, especially the vegetated ones, present along almost the entire beachfront, some of which still maintaining the dune-beach equilibrium, were confirmed as crucial elements for controlling erosional processes. The coastal vulnerability analysis demonstrated an evident mitigation of the exposure index due to the presence of these dune features, emphasizing their protective function. The coastal vulnerability analysis allowed the conclusion that the factors influencing the coast's exposure to erosive effects are multifactorial and interrelated. For the studied area, the most impactful variables in the classification of coastal vulnerability to erosion were the geomorphology of the coast, the incidence of waves and winds, and the presence of dunes.

Given these results, the anthropogenic occupation of beachfront areas — environments highly targeted by socioeconomic interest, particularly from the civil construction and tourism industries—must be intrinsically accompanied by rigorous environmental assessments, strategic coastal management actions, and the implementation of effective environmental control measures. Such actions aim to foster more sustainable solutions for these ecosystems, which still preserve natural characteristics with the potential to mitigate and adapt to the challenges of climate change.

Author Contributions: G.D.R.C.: Conception, Methodology, Formal analysis, Investigation, Writing – original draft, Writing – review and editing. V.E.A.: Conception, Investigation, Writing – review and editing, Supervision, Project administration. L.R.S.G.P.: Formal analysis, Writing – review and editing. N.S.Z.: Conception, Writing – review and editing.

Conflict of Interest: The authors declare no conflict of interest. The funders had no interference in the development of the study; in the collection, analysis, or interpretation of the data; in the writing of the manuscript, or in the decision to publish the results.

Acknowledgments: This work is a contribution to the research themes of the National Institute of Science and Technology – KLIMAPOLIS, funded by the National Council for Scientific and Technological Development (CNPq) and the Brazilian Ministry of Science, Technology and Innovation (MCTI). We thank the Graduate Program in Civil and Environmental Engineering (PPCIVAM) at the Federal University of Rio Grande do Norte (UFRN), within which this work was developed, and especially Professor Ada Scudelari for her contributions. We also thank Dr. Maria de Fátima Alves de Matos for her guidance, suggestions, and contributions to the development of this study. Our thanks extend to the Civil Defense of the State of Rio Grande do Norte and to the Institute for Sustainable Development and Environment of Rio Grande do Norte (IDEMA), especially Cintia Brito Prudente da Silva, for the insights on the challenges of the region that became the focus of this study. Finally, we thank the Ecoeng team, who, in various ways, provided inspiration, support, and tools for the development of this research.

7. References

1. ADDO, K. K.; JAYSON-QUASHIGAH, P.-N.; KUFOGBE, S. Quantitative Analysis of Shoreline Change Using Medium Resolution Satellite Imagery in Keta, Ghana. Marine Sciences, v. 1, p. 1–9, 2011. DOI: 10.5923/j.ms.20110101.01
2. ALMEIDA, L. P.; OLIVEIRA, I. E. D; LYRA, R.; DAZZI, R. L. S; MARTINS, V. G.; KLEIN, A. H. F. D. F**.** Coastal Analyst System from Space Imagery Engine (CASSIE): shoreline management module. **Environmental Modelling & Software,** v. 140, 2021. DOI: 10.1016/j.envsoft.2021.105033
3. AMARO, V. E.; GOMES, L. R. S.; LIMA, F. G. F. D; SCUDELARI, A. C.; NEVES, C. F.; BUSMAN, D. V.; SANTOS, A. L. S. Multitemporal Analysis of Coastal Erosion Based on Multisource Satellite Images, Ponta Negra Beach, Natal City, Northeastern Brazil. **Marine Geodesy**, v. 38, n. 1, p. 1–25, 2015. DOI: 10.1080/01490419.2014.904257
4. AMARO, V. E.; CARVALHO, R. C.; MATOS, M. F. A.; INGUNZA, M. D. P. D; SCUDELARI, A. C. Avaliação da suscetibilidade do solo à erosão nas falésias do litoral oriental do estado do Rio Grande do Norte. **Revista Brasileira de Geomorfologia**, v. 22, n. 1, p. 3–25, 2021a. DOI: 10.20502/RBG.V22I1.1887
5. AMARO, V. E.; SCUDELARI, A. C.; OLIVEIRA, D. S. D; LACERDA, I. L. C; MATOS, M. F. A. Analysis of physical vulnerability indices using geotechnologies in the Barreira do Inferno region of Rio Grande do Norte state, Brazil. **Revista de Geociências do Nordeste**, v. 7, n. 2, p. 179–192, 2021. DOI: 10.21680/2447-3359.2021v7n2ID22034
6. ARAÚJO, R. V.; PEREIRA, P. S.; LINO, A. P.; ARAÚJO, T. M.; GONÇALVES, R. M. Morphodynamic study of sandy beaches in a tropical tidal inlet using RPAS. **Marine Geology**, v. 438, 2021. DOI: 10.1016/j.margeo.2021.106540
7. ARKEMA, K. K.; GUANNEL, G.; VERUTES, G.; WOOD, S. A.; GUERRY, A.; RUCKELSHAUS, M.; KAREIVA, P.; LACAYO, M.; SILVER, J. M. Coastal habitats shield people and property from sea-level rise and storms. **Nature Climate Change**, v. 3, n. 10, p. 913–918, 2013. DOI: 10.1038/nclimate1944
8. BOOIJ, N.; RIS, R. C.; HOLTHUIJSEN, L. H. A third-generation wave model for coastal regions 1. Model description and validation. **Journal of Geophysical Research: Oceans**, v. 104, n. C4, p. 7649–7666, 1999. DOI: 10.1029/98JC02622
9. BRASIL. Projeto Orla: fundamentos para gestão integrada. MP/SPU, 2002.
10. BRASIL. MARINHA. DIRETORIA DE HIDROGRAFIA E NAVEGAÇÃO (DHN). **Carta náutica n.º 21900 – Da Ponta Maceió ao Cabo Calcanhar**. Niterói: DHN, 2022. Escala 1:350.000.
11. BUSMAN, D. V.; AMARO, V. E.; SOUZA-FILHO, P. W. M. Análise estatística multivariada de métodos de vulnerabilidade física em zonas costeiras tropicais. **Revista Brasileira de Geomorfologia**, v. 17, n. 3, 2016. DOI: 10.20502/rbg.v17i3.912
12. CAMUS, P.; MÉNDEZ, F. J.; MEDINA, R.; TOMAS, A.; IZAGUIRRE, C. High resolution downscaled ocean waves (DOW) reanalysis in coastal areas. **Coastal Engineering**, v. 72, p. 56–68, 2013. DOI: 10.1016/j.coastaleng.2012.09.002
13. CHAPMAN, D. M. Zetaform bays. In: SCHWARTZ, M. (Ed.). Beaches and Coastal Geology. New York, NY: Springer US, 1984. p. 883–885.
14. CHARLIER, R. H.; MEYER, C. P. D. Coastal erosion: response and management. Springer, Berlin, 343 p. 1998.
15. CHEN, C. T. A.; GAO, X.; ISHIZAKA, J.; LEBEL, L. Coastal seas in a changing world: Anthropogenic impact and environmental responses. **Continental Shelf Research**, v. 111, p. 109–111, 2015. DOI: 10.1016/j.csr.2015.11.007
16. COSTA, W. F.; FONSECA, M. A. P. Lazer, turismo, especulação imobiliária e conflito territorial entre São Miguel do Gostoso e Touros (RN). **Revista Brasileira de Pesquisa em Turismo**, v. 13, n. 3, p. 92–104, 2019. DOI: 10.7784/rbtur.v13i3.1587
17. CPRM (Companhia de Pesquisa de Recursos Minerais). **Projeto cadastro de fontes de abastecimento por água subterrânea. Diagnóstico do município de São Miguel de Touros, estado do Rio Grande do Norte.** Recife: CPRM, 2005.
18. CPRM (Companhia de Pesquisa de Recursos Minerais). **Geologia e recursos minerais do estado do Rio Grande do Norte - escala 1:500.000**. Organizador: Luiz Alberto de Aquino Angelim – Recife/PE. Serviço Geológico do Brasil. 2007.
19. DAUD, S.; MILOW, P.; ZAKARIA, R. Analysis of Shoreline Change Trends and Adaptation of Selangor Coastline, Using Landsat Satellite Data. **Journal of the Indian Society of Remote Sensing**, v. 49, 2021. DOI: 10.1007/s12524-020-01218-0
20. DINIZ, M. T. M.; OLIVEIRA, G. P. D; MAIA, R. P.; FERREIRA, B. Mapeamento geomorfológico do estado do Rio Grande do Norte. **Revista Brasileira de Geomorfologia**, v. 18, n. 4, p. 689–701, 2017. DOI: 10.20502/rbg.v18i4.1255
21. DINIZ, M. T. M.; PEREIRA, V. H. C. Climatologia do estado do Rio Grande do Norte, Brasil: sistemas atmosféricos atuantes e mapeamento de tipos de clima. **Boletim Goiano de Geografia**, v. 35, p. 488–506, 2015.
22. EMPARN (Empresa de Pesquisa Agropecuária do Rio Grande do Norte). **Meteorologia – Dados pluviométricos estação TELEPLU – São Miguel do Gostoso**. 2022.
23. EUROPEAN SPACE AGENCY (ESA). **Copernicus Browser: Sentinel-2 imagery**. Paris: ESA, 2023. Disponível em: https://browser.dataspace.copernicus.eu/. Accessed in December 2023.
24. FORGIARINI, A. P. P.; AMARAL DE FIGUEIREDO, S.; CALLIARI, L. J.; GOULART, E. S.; MARQUES, W.; TROMBETTA, T. B.; OLEINIK, P. H.; GUIMARÃES, R. C.; ARIGONY-NETO, J.; CABRAL SALAME, C. Quantifying the geomorphologic

and urbanization influence on coastal retreat under sea level rise. **Estuarine, Coastal and Shelf Science**, v. 230, p. 106437, 15 dez. 2019. DOI: 10.1016/j.ecss.2019.106437

25. GONZÁLEZ, M.; NICLODI, K. L.; GUTIÉRREZ, O. Q.; CÁNOVAS, V.; ESPEJO, A. Processos costeiros brasileiros: ventos, clima de ondas e nível do mar com base em reanálise de dados. In: **Sistema de Modelagem Costeira do Brasil – Estudos de Caso**, p. 11–64, 2018.
26. GORNITZ, V. **Vulnerability of the East Coast, U.S.A. to future sea level rise.** Journal of Coastal Research, p. 201–237, 1990.
27. GRIGIO, A. M.; DE CASTRO, A. F.; SOUTO, M. V. S.; AMARO, V. E.; VITAL, H.; DIODATO, M. A. Use of Remote Sensing and GIS in the Determination of the Natural and Environmental Vulnerability of the Municipal District of Guamaré – Rio Grande do Norte – Northeast of Brazil. **Journal of Coastal Research**, p. 1427–1431, 2006. Disponível em: http://www.jstor.org/stable/25742990
28. GUANNEL, G.; ARKEMA, K.; RUGGIERO, P.; VERUTES, G. The power of three: Coral reefs, seagrasses and mangroves protect coastal regions and increase their resilience. **PLoS ONE**, v. 11, n. 7, 2016. DOI: 10.1371/journal.pone.0158094
29. HAMMAR-KLOSE, E. S.; THIELER, E. R.; U.S. GEOLOGICAL SURVEY. **Coastal vulnerability to sea-level rise: a preliminary database for the U.S. Atlantic, Pacific, and Gulf of Mexico coasts.** U.S. Geological Survey Data Series DDS-68, 2001. DOI: 10.3133/ds68
30. HENNIG, T. Damming the transnational Ayeyarwady basin. Hydropower and the water-energy nexus. **Renewable and Sustainable Energy Reviews**, v. 65, p. 1232–1246, 2016. DOI: 10.1016/j.rser.2016.07.048
31. HIMMELSTOSS, E. A. et al. **Digital Shoreline Analysis System (DSAS) version 5.0 user guide Open-File Report.** Reston, VA: [s.n.], 2018. Disponível em: <https://pubs.usgs.gov/publication/ofr20181179>.
32. IBGE (Instituto Brasileiro de Geografia e Estatística). **Censo Brasileiro 2010.** 2010.
33. IBGE (Instituto Brasileiro de Geografia e Estatística). **Manual técnico da vegetação brasileira.** 2ª ed. Rio de Janeiro: IBGE, 2012.
34. IBGE (Instituto Brasileiro de Geografia e Estatística). **Base de Dados Espacial Brasil Versão 2019**. Escala 1:250.000, 2019.
35. IBGE (Instituto Brasileiro de Geografia e Estatística). **Censo Brasileiro 2022.** 2022.
36. INSTITUTO NACIONAL DE PESQUISAS ESPACIAIS (INPE). **Catálogo de Imagens CBERS**. São José dos Campos: INPE, 2023. Disponível em: https://www.dgi.inpe.br/CDSR/. Accessed in December 2023.
37. IPCC (Intergovernmental Panel on Climate Change). **Climate change 2014: synthesis report: longer report.** Cambridge: Cambridge University Press, 2014.
38. JUVINO DA SILVA, L. R.; AMARO, V. E.; SCUDELARI, A. C.; PINHEIRO, L. R. S. G. Risk map of coastal erosion and gravitational mass movements of the Brazilian eastern coast: a case study of Pipa Beach/RN. **Revista Brasileira de Geomorfologia**, v. 24, n. 2, 2023. DOI: 10.20502/rbg.v24i2.2281
39. LACERDA, I. L. C; AMARO, V. E.; MATOS, M. F. A.; SCUDELARI, A. C. Physical vulnerability of the coastal zone under wind farms influence of the cities of Pedra Grande and São Miguel do Gostoso/RN, Brazil. **Revista Brasileira de Ciências Ambientais**, v. 57, n. 3, p. 422–433, set. 2022. DOI: 10.5327/z2176-94781244
40. LOEW, A.; BELL, W.; BROCCA, L.; BULGIN, C. E.; BURDANOWITZ, J.; CALBET, X.; DONNER, R. V.; GHENT, D.; GRUBER, A.; KAMINSKI, T.; KINZEL, J.; KLEPP, C.; LAMBERT, C.; SCHAEPMAN-STRUB, G.; SCHRÖDER, M.; VERHOELST, T. Validation practices for satellite-based Earth observation data across communities. **Reviews of Geophysics**, 55(3), 779-817, 2017. https://doi.org/10.1002/2017RG000562
41. LUIJENDIJK, A.; HAGENAARS, G.; RANASINGHE, R.; BAART, F.; DONCHYTS, G.; AARNINKHOF, S. The State of the World's Beaches. **Scientific Reports**, v. 8, n. 1, 2018. DOI: 10.1038/s41598-018-24630-6
42. MACEDO, Y.; SILVA, E.; OLIVEIRA, V.; JÚNIOR, J.; COSTA, D.; CESTARO, L. Serviços ambientais das unidades geoambientais no município de São Miguel do Gostoso/RN, Brasil. **GOT – Journal of Geography and Spatial Planning**, v. 12, p. 205–229, 2017. DOI: 10.17127/got/2017.12.009
43. MARINHA DO BRASIL. **Carta Náutica 21900 da Marinha do Brasil: Da ponta Maceió ao Cabo Calcanhar.** Escala 1:300.000. (s.d.)
44. MARRONI, E. V.; ASMUS, M. L. **Gerenciamento Costeiro: uma proposta para o fortalecimento comunitário na gestão ambiental.** Pelotas: Editora USEB, 2005.
45. MATIAS, E. M. S. **Microrrealidades transformadas pelo turismo em São Miguel do Gostoso – RN.** Tese (Doutorado em Ambiente e Sociedade) - Programa de Pós-Graduação em Ambiente e Sociedade, Universidade Estadual de Campinas, Campinas. 2017. 167p.
46. MATOS, M. F. A.; AMARO, V. E.; SCUDELARI, A. C.; ROSADO, S. B. Estimation of long term shoreline changes along the Eastern Coast of Rio Grande do Norte State, Northeast Brazil. **Revista Brasileira de Geomorfologia**, v. 23, n. 1, p. 1027–1053, 2022a. DOI: 10.20502/RBG.V23I1.1953

47. MATOS, M. F. A; SCUDELARI, A. C; AMARO, V. E. Variabilidade Interanual do Potencial Energético das Ondas Oceânicas na Costa Setentrional do Rio Grande do Norte, Atlântico Equatorial Sul. **Anuário do Instituto de Geociências**, Rio de Janeiro, v. 45, 2022b. DOI: 10.11137/1982-3908_2022_45_46460.
48. MELO, A. B. C.; CAVALCANTI, I. F.; SOUZA, P. P. Zona de Convergência Intertropical do Atlântico**.** In: CAVALCANTI, I. F. A. (Ed.), **Tempo e clima no Brasil**, cap. 2, p. 25–41. São Paulo: Oficina de Textos, 2009.
49. MOURA, J. E. **Influência dos modelos digitais de terreno na modelagem de circulação hidrodinâmica 2DH: um estudo de caso.** Dissertação (Mestrado em Engenharia Sanitária) - Programa de Pós-Graduação em Engenharia Sanitária, Universidade Federal do Rio Grande do Norte, Natal. 2010. 137p.
50. MUEHE, D. (org.). **Panorama da Erosão Costeira no Brasil.** Brasília: Ministério do Meio Ambiente, 2018.
51. MUEHE, D.; KLUMB-OLIVEIRA, L. Deslocamento da linha de costa versus mobilidade praial. **Quaternary and Environmental Geosciences**, v. 5, n. 2, 31 dez. 2014.
52. NOARDO, F. Multisource spatial data integration for use cases applications. **Transactions in GIS**, v. 26, n. 7, p. 2874-2913, 2022. DOI: 10.1111/tgis.12987.
53. OTSU, N. A threshold selection method from gray-level histograms. **IEEE Transactions on Systems, Man, and Cybernetics**, v. 9, n. 1, p. 62–66, 1979. DOI: 10.1109/TSMC.1979.4310076
54. PARKER, B. B. The difficulties in measuring a consistently defined shoreline? The problem of vertical referencing. **Journal of Coastal Research**, v. 38, p. 44–56, 2003.
55. PFALTZGRAFF, P. A. S.; TORRES, F. S. M. **Geodiversidade do estado do Rio Grande do Norte**. CPRM, 2010.
56. PINHEIRO, L. R. S. G.; SOUZA, R. F.; AMARO, V. E.; SPYRIDES, M. H. C. 40 Years Extreme Offshore Waves off the Eastern Continental Shelf of Rio Grande do Norte, Northeast Brazil. **Revista Brasileira de Geografia Física**, v. 16, n. 2, p. 1040-1059, 2023. DOI: 10.26848/rbgf.v16.2.p1040-1059
57. POLLARD, J. A.; SPENCER, T.; BROOKS, S. M. The interactive relationship between coastal erosion and flood risk. **Progress in Physical Geography: Earth and Environment**, v. 42, n. 4, p. 556–578, 2019. DOI: 10.1177/0309133318790089.
58. POLLOCK, W.; WARTMAN, J. Human vulnerability to landslides. **GeoHealth**, v. 4, n. 10, 2020. DOI: 10.1029/2020GH000287
59. PRUDÊNCIO, M. C.; AMARO, V. E.; SCUDELARI, A. C. Coastal evolution analysis between the years 1984 and 2014 of a stretch of Rio Grande do Norte eastern coast, northeast Brazil. **Anuário do Instituto de Geociências – UFRJ**, v. 42, n. 4, p. 189–205, 2019. DOI: 10.11137/2019_4_189_205
60. QUETZALCÓATL, O.; GONZÁLEZ, M.; CÁNOVAS, V.; MEDINA, R.; ESPEJO, A.; KLEIN, A.; TESSLER, M. G.; ALMEIDA, L. R.; JARAMILLO, C.; GARNIER, R.; KAKEH, N.; GONZÁLEZ-ONDINA, J. SMCε, a coastal modeling system for assessing beach processes and coastal interventions: Application to the Brazilian coast. **Environmental Modelling & Software**, v. 116, p. 131–152, 2019. DOI: 10.1016/j.envsoft.2019.03.001
61. REBOITA, M. S.; AMBRIZZI, T.; DA ROCHA, R. P. Entendendo o tempo e o clima na América do Sul. **Terrae Didatica**, v. 8, n. 1, p. 34–50, 2012.
62. SMG (São Miguel do Gostoso). **Histórico [página eletrônica]**. Disponível em: < https://site.saomigueldogostoso.rn.gov.br/pages/historico>. Accessed in June 2025.
63. SANTOS, M. S. T.; AMARO, V. E.; SOUTO, M. V. S. Metodologia geodésica para levantamento de linha de costa e modelagem digital de elevação de praias arenosas em estudos de precisão de geomorfologia e dinâmica costeira. **Revista Brasileira de Cartografia**, v. 63, 2011. DOI: 10.14393/rbcv63n0-43760
64. SOUZA, P.; CAVALCANTI, I. F. A. **Atmospheric centres of action associated with the Atlantic ITCZ position.** International Journal of Climatology, v. 29, n. 14, p. 2091–2105, 2009. DOI: 10.1002/joc.1823
65. TAVEIRA, M. S. **Turismo e comunidades de praia: São Miguel do Gostoso no caminho do mar e na direção dos ventos.** Tese (Doutorado em Ciências Sociais) - Programa de Pós-Graduação em Ciências Sociais, Universidade Federal do Rio Grande do Norte, Natal. 2015. 363p.
66. THIELER, E. R.; HIMMELSTOSS, E. A.; ZICHICHI, J. L.; ERGUL, A.; U.S. GEOLOGICAL SURVEY. **Digital Shoreline Analysis System (DSAS) Version 4.0 – an ArcGIS extension for calculating shoreline change.** U.S. Geological Survey Open-File Report, 2009. DOI: 10.3133/ofr20081278
67. TOLMAN, H. L. **User manual and system documentation of WAVEWATCH III version 3.14.** U.S. Department of Commerce / NOAA/NWS/NCEP, Camp Springs, MD, 2009.
68. UNITED STATES GEOLOGICAL SURVEY (USGS). Shuttle Radar Topography Mission (SRTM) – Digital Elevation Model. Sioux Falls: USGS, 2023. Disponível em: https://earthexplorer.usgs.gov/. Accessed in December 2023.
69. VOUSDOUKAS, M. I.; RANASINGHE, R.; MENTASCHI, L.; PLOMARITIS, T. A.; ATHANASIOU, P.; LUIJENDIJK, A.; FEYEN, L. Sandy coastlines under threat of erosion. **Nature Climate Change**, v. 10, n. 3, p. 260–263, 2020. DOI: 10.1038/s41558-020-0697-0

70. WANNEWITZ, M.; AJIBADE, I.; MACH, K. J.; MAGNAN, A.; PETZOLD, J.; RECKIEN, D.; ULIBARRI, N.; AGOPIAN, A.; CHALASTANI, V. I.; HAWXWELL, T.; HUYNH, L. T. M.; KIRCHHOFF, C. J.; MILLER, R.; MUSA-SURUGU, J. I.; NAGLE ALVERIO, G.; NIELSEN, M.; NUNBOGU, A. M.; PENTZ, B.; REIMUTH, A.; … GARSCHAGEN, M. Progress and gaps in climate change adaptation in coastal cities across the globe. **Nature Cities**, v. 1, n. 9, p. 610–619, 26 ago. 2024. DOI: 10.1038/s44284-024-00106-9
71. ZAMBONI, N. S.; MATOS, M. F. A.; AMARO, V. E.; PRUDÊNCIO, M. C.; CARVALHO, A. R. The protective role of mangroves in safeguarding coastal populations through hazard risk reduction: a case study in northeast Brazil. **Ocean and Coastal Management**, v. 229, 2022. DOI: 10.1016/j.ocecoaman.2022.106353
72. ZAMBONI, N. S.; MATOS, M. F. A. de; AMARO, V. E.; PRUDÊNCIO, M. C.; VERUTES, G. M.; CARVALHO, A. R. Impacts of land use change on mangrove blue carbon services: a future perspective in northeastern Brazil. **Estuarine, Coastal and Shelf Science**, v. 317, p. 109185, jun. 2025. DOI: 10.1016/j.ecss.2025.109185